

学位論文

Studies on the roles of external strain in the regulatory mechanism of
dynein activity underlying flagellar oscillation in sea urchin sperm

(ウニ精子鞭毛の振動運動を誘起するダイニンの外力に依存した活性制御)

平成 29 年 10 月 博士（理学）申請

東京大学大学院理学系研究科
生物科学専攻

餘家 博

Acknowledgements

I thank my thesis advisor, Dr. Chikako Shingyoji for giving me thoughtful advice throughout this work. I also thank the director and the staff of the Misaki Marine Biological Station, the University of Tokyo, and the Research Center for Marine Biology, Tohoku University, for supplying sea urchins. I thank The Company of Biologist Limited for providing permission to reproduce the article in Journal of Experimental Biology of which I am an author (Yoke and Shingyoji, 2017), which constitute a part of the Abstract, a part of the General Introduction and most part of the Chapter I of this thesis. Lastly, I thank my family for their warm support throughout this study.

Abstract

Oscillatory bending movement of eukaryotic flagella is powered by orchestrated activity of dynein motor proteins that hydrolyze ATP and produce microtubule sliding. Although the ATP concentration within a flagellum is kept uniform at a few millimoles per litre level, sliding activities of dyneins are dynamically coordinated along the flagellum in accordance with the phase of bending waves. Thus, at the organellar level the dynein not only generates force for bending but also modulates its motile activity by responding to bending of the flagellum. Single molecule analyses have suggested that dynein at the molecular level, even if isolated from the axoneme, could alter the modes of motility in response to mechanical strain. However, it still remains unknown whether the coordinated activities of multiple dyneins can be modulated directly by mechanical signals. In this thesis, I studied the effects of externally applied strain imposed by micromanipulation with a glass microneedle on the sliding movement of microtubules interacted with ensemble of dynein molecules isolated from the intact axonemal structure. In the Chapter I, I investigated the effects of external strain on microtubule sliding induced by isolated outer arm dyneins adsorbed on a glass surface. I found that three modes of motility that have not been previously characterized without bending can be induced: stoppage, backward sliding and dissociation. Sliding velocities also changed with imposed bending. These results suggest that the activity of ensemble of isolated dyneins on a glass surface are modified and coordinated in a quite flexible manner. In the Chapter II, I also investigated the effects of imposed bending on the sliding movement of microtubules interacted with dyneins still attached on doublet microtubules obtained from sea urchin sperm flagella. I found that bending in different

regions of microtubules can affect the relative frequency of the microtubules that do not show sliding after imposed bending. This result suggests that dyneins may have the ability to respond to mechanical signals also when they are arrayed on a doublet microtubule, as in *in vivo* flagella. These results together suggest that the activities of ensemble of dyneins interacted with a microtubule are modified and coordinated through external strain in a quite flexible manner, and that such a regulatory mechanism may be the basis of flagellar oscillation.

Abbreviations

CP: central-pair microtubules

RS: radial spokes

EGTA: glycoetherdiamine-*N, N, N', N'*-tetra-acetic acid

DTT: dithiothreitol

PIPES: 1,4-piperazinediethanesulfonic acid

MES: 2-(*N*-morpholino)ethanesulfonic acid

MT: (singlet) microtubule

Fw: forward sliding

Bw: backward sliding

HEPES: 4-(2-hydroxyethyl)-1-piperazineethanesulfonic acid

EDTA: ethylenediamine-*N, N, N', N'*-tetraacetic acid-dipotassium salt, dihydrate

DMT: doublet microtubule

Table of Contents

Acknowledgements	ii
Abstract	iii
Abbreviations	v
General Introduction	1

Chapter I

Effects of external strain on the regulation of microtubule sliding induced by outer arm dyneins adsorbed on a glass surface

Abstract	8
Introduction	9
Materials and Methods	11
Results	15
Microtubule sliding induced by dyneins in the open surface chamber	15
Planar bending of sliding microtubules induced forward sliding and stoppage	16
Decrease in sliding velocity induced by planar bending	18
Stoppage of sliding was reversible	19
Conditions required for induction of stoppage	20
Backward sliding induced by continuous backward strain	23
Three-dimensional effects caused dissociation	25
Discussion	27
Induction of a stationary mode of dynein	27

Bidirectionality	28
Decrease in sliding velocity	29
Strain-dependent regulation of outer arm dynein in an axoneme	30
Table 1-1	32
Figures and Legends (1-1 – 1-9)	33

Chapter II

Exploration on the method: an attempt on investigating the effects of imposed bending on the microtubule sliding induced by dyneins on the doublet microtubules

Abstract	52
Introduction	53
Materials and Methods	55
Results and Discussion	59
Microtubule sliding induced by dyneins arrayed on the doublet microtubules	59
Responses of the microtubules induced by the 2nd UV flash after imposed bending	60
Table 2-1	63
Figures and Legends (2-1 – 2-3)	64
General Discussion	70
References	78

General Introduction

Historical background of flagellar oscillation: inter-doublet sliding induced by dyneins

Flagella and cilia in eukaryotes show coordinated oscillatory movements. Oscillation of cilia and flagella is powered by a motor protein, axonemal dynein (hereafter called dynein), which is an ATPase protein arrayed on each of the nine outer doublet microtubules within a cilium or a flagellum (Gibbons and Rowe, 1965). Studies have established that cyclical bending of cilia and flagella is the result of ATP-dependent sliding movements between the doublet microtubules induced by dyneins (“sliding filament model”), rather than the result of contraction of the filaments within a flagellum. Observation of the axonemes with electron micrographs showed that the lengths of the microtubules in a cilium are constant during beating, supporting the sliding filament model (Satir, 1968), and the study on movements of multiple beads attached to doublet microtubules of demembrated sperm flagella showed that the movements of the beads were in accordance with the sliding filament model (Brokaw, 1989). The existence of sliding induced by dyneins and its importance in producing bends of the axonemes were further verified by the observation that axonemes digested with trypsin shows ATP-dependent sliding disintegration into individual microtubules (Summers and Gibbons, 1971), and by the observation that localized application of ATP to demembrated sperm flagellum by iontophoresis induces bending of the flagellum (Shingyoji et al, 1977). The polarity of the sliding activity of dyneins on microtubules was revealed as minus-end directed by the electron microscopic observations of sliding disintegration of the axonemes, in which a doublet microtubule slid in a single direction relative to its neighbor (Sale and Satir, 1977; Fox and Sale, 1987).

For the flagellar oscillation, the amount and the velocity of sliding induced by

dyneins must be regulated in a coordinated manner, among the nine doublet microtubules, along the flagellum, and according to the phase of the propagating wave (Gibbons, 1981). This regulation cannot be attributed to local changes in the ATP concentrations within a flagellum because flagellar axonemes demembrated with detergent, such as those of sea urchin spermatozoa, are still able to beat cyclically in the presence of ATP and Mg^{2+} (Gibbons and Gibbons, 1972).

Roles of mechanical signals in the regulation of dynein activities in axonemes

How are the dynein activities regulated and coordinated? Studies have suggested that in the 9+2 structure (nine outer doublet microtubules surrounding the two central-pair microtubules) of a flagellum, the sliding activities of dynein can be modulated by external strain or bending imposed to the axoneme. Okuno and Hiramoto investigated the responses of starfish sperm flagella to mechanical stimulations and showed that when the tip of a microneedle was attached to the middle region of a beating sperm flagellum, the propagation of the bending waves to the distal regions beyond the point of attachment was inhibited in a reversible manner, suggesting that mechanical signals transduced from proximal regions of the axoneme is responsible for the propagation of the bending waves to the more distal regions (Okuno and Hiramoto, 1976). Experiments on the effects of imposed head vibration to sea urchin live spermatozoa showed that the beat plane, beat frequency and sliding velocity, which are thought to reflect the dynein activities, can be modified by mechanical signals (Gibbons et al., 1987; Shingyoji et al., 1991). Also, the experiments on the effects of imposed bending on the sliding movements of elastase-treated sperm flagellar axonemes showed that changes in sliding velocities and switching of active dynein arrays can be induced by imposed bending

(Morita and Shingyoji, 2004; Hayashi and Shingyoji, 2008). Based on these results, the idea of the “feedback regulation” of dynein in the axoneme is well accepted, in which the inter-doublet sliding induced by dynein results in the bending of the axoneme and the bending regulates the dynein activities in turn. Then the question is how the bending regulates dynein activity.

Importance of the central-pair microtubules

The axonemal sub-structures such as the central-pair microtubules (CP) and the radial spokes (RS) may mediate the feedback regulation of dynein. CP and RS have been suggested to be dispensable for the basic mechanism of beating itself; at low ATP concentrations (e.g. $<100 \mu\text{mol l}^{-1}$) (Omoto et al., 1996; Frey et al., 1997) and in the presence of high salts and organic compounds (Yagi and Kamiya, 2000), some mutant axonemes that lack CP or RS are able to beat, and there are reports of motile cilia and flagella that naturally lack CP (Prensier et al., 1980; Nonaka et al., 1998). However, at normal ATP concentrations (e.g. $>100 \mu\text{mol l}^{-1}$ or 1 mmol l^{-1}), CP and RS are likely to be involved in the regulation of microtubule sliding and wave forms (Hosokawa and Miki-Noumura, 1987; Smith and Sale, 1992; Smith, 2002; Wargo and Smith, 2003; Nakano et al., 2003). Also, there is a hypothesis that bending of the axoneme may regulate dynein activity through mechanical signal imposed on RS (Porter and Sale, 2000; Oda et al., 2014). Thus, in a physiological condition, the 9+2 structure is thought to be responsible for regulating dynein activities to some extent.

Self-regulatory nature of dynein

The role of the 9+2 structure for regulation of dynein does not exclude the possibility of

involvement of the dynein molecules themselves in the strain-dependent cyclical bending. In theoretical works, the strain has been hypothesized to work in the direction either perpendicular to the length of the microtubule as the distortion of the axoneme (transverse force; t-force) (Lindemann, 1994a; Lindemann, 1994b) or parallel to the microtubule as the elastic and viscous resistance (Brokaw, 1975; Riedel-Kruse et al., 2007). These models typically assume strain-dependent detachment of dyneins from the adjacent doublet microtubules, and are able to reproduce the oscillatory movement of flagella.

In experimental works, single molecule analyses of dynein using an optical trap have revealed strain-dependent backward stepping (toward the plus-end of microtubules) (Shingyoji et al., 1998) and strain-dependent backward force generation (Shingyoji et al., 2015) of dynein. These results suggest that a single dynein molecule can change modes of sliding activities (from the forward mode to the backward mode) in response to external strain that is parallel to the microtubule. However, when dyneins on a doublet microtubule work in a flagellum, they usually function as a team of hundreds of molecules, and in general, behavior of ensemble of motor proteins is not necessarily a simple summation of that of a single motor protein, a counterexample of which is the directionality of kinesin 5 motors, Cin8 and Kip1 (Roostalu et al., 2011; Fridman et al., 2013). Therefore, it is still a mystery whether the collective activities of ensemble of dynein molecules can also be regulated and coordinated by mechanical signals, and if it is the case, a question of what kinds of modes of motility they may have remains unsolved.

The plan of this thesis

In this thesis, to test whether ensemble of dynein molecules have the ability to respond to mechanical signals, the effects of externally applied strain on the sliding movement of microtubules interacted with ensemble of dynein molecules isolated from the intact axonemal structure were studied. In the Chapter I, the effects of mechanical manipulations on the sliding movements of microtubules interacted with isolated outer arm dyneins (21S dyneins) adsorbed on a glass surface were investigated. I found that dissociation and stoppage of sliding were induced by external strain. I also found that backward sliding, which has been observed in single molecule analyses (Shingyoji et al., 2015), can also be induced in this multiple-motor assay. Sliding velocities also changed with imposed bending. These results suggest that the activity of ensemble of isolated dyneins on a glass surface are modified and coordinated in a quite flexible manner. In the Chapter II, I explored on a new experimental system in which effects of imposed bending on sliding movements of microtubules interacted with dyneins still attached on the doublet microtubules of sea urchin sperm axonemes can be investigated. I have not found any differences between behaviour of microtubules with imposed bending and that without one in this experimental system, but I found that imposed bending in different regions of microtubules could affect the modes of motility (the sliding mode and the stationary mode) of dyneins. This result suggests that dyneins may have the ability to respond to mechanical signals when they are still attached to the doublet microtubules as in the *in vivo* flagella. Together, these results suggest that sliding activities of ensemble of dynein molecules are modified and coordinated through external strain in a flexible manner, and that this regulatory mechanism may be an important basis of flagellar oscillation.

Chapter I

**Effects of external strain on the regulation of microtubule sliding
induced by outer arm dyneins adsorbed on a glass surface**

Abstract

Dyneins are responsible for the flagellar oscillation through producing orchestrated sliding movements between the doublet microtubules in the axoneme, and studies have suggested that mechanical signals seem to be the key to the regulation of the activities of dyneins in flagella. Single molecule analyses of dynein have suggested that dynein at the molecular level, even if isolated from the axoneme, could alter the modes of motility in response to mechanical strain. However, it still remains unknown whether the coordinated activities of multiple dyneins can be modulated directly by mechanical signals. Here, I studied the effects of externally applied strain on the sliding movement of microtubules interacted with an ensemble of dynein molecules adsorbed on a glass surface in the presence of 1 mmol l^{-1} ATP. I found that by bending the microtubules with a glass microneedle, three modes of motility that have not been previously characterized without bending can be induced: stoppage, backward sliding and dissociation. Modification in sliding velocities was also induced by imposed bending. These results suggest that the activities of dyneins interacted with a microtubule can be modified and coordinated through external strain in a quite flexible manner, and that such a regulatory mechanism may be the basis of flagellar oscillation.

Introduction

Do the dyneins themselves, isolated from the axonemal structures, still have the ability to respond to mechanical signals? Previous studies on single molecule analyses suggested that single molecule dynein can change modes of motility from the forward mode to the backward in response to mechanical signals (Shingyoji et al., 1998; Shingyoji et al., 2015). However, it is still unknown whether ensemble of dynein molecules isolated from the axoneme can modify the collective sliding activity in response to mechanical signals.

The simplest and most prevalent assay system to study the activity of ensemble of motor proteins *in vitro* is the so-called ‘*in vitro* motility assay’, in which motor proteins adsorbed on a glass surface translocate the complementary purified filaments (Vale et al., 1985; Kron and Spudich, 1986; Vale and Toyoshima, 1988). It has been broadly used to study the properties of dynein, such as sliding velocity, duty ratio, modes of interaction with microtubules, and the effects of inhibitors or nucleotides (Vale et al., 1989; Moss et al., 1992; Hamasaki et al., 1995; Sakakibara et al., 1999; Inoue and Shingyoji, 2007; Kotani et al., 2007). Investigating the effect of external strain on dynein in this assay system has been technically difficult, and only shift in sliding velocity has been reported as the effect of small external force applied by fluid flow imposed to a sliding microtubule interacted with *Chlamydomonas* inner arm dynein species c (Kikushima and Kamiya, 2009). Here, I developed a new assay system with introduction of micromanipulation techniques based on the *in vitro* motility assay, in which sliding microtubules can be freely bent with a glass microneedle, and the direction of the strain imposed on dynein and microtubules can be estimated from the

shapes and motion of the microtubules. I found that dissociation and stoppage of sliding microtubules were induced by external strain. I also found that backward sliding, which has been observed in single molecule analyses (Shingyoji et al., 2015), can also be induced. Modification in sliding velocities was also observed. These results suggest that sliding activities of multiple dynein molecules can be modified and coordinated through external strain in a flexible manner, and that this regulatory mechanism might be involved in the flagellar oscillation.

A part of the Abstract, a part of the Introduction, all of the Materials and Methods, all of the Results (including all tables, figures and legends) and all of the Discussion in the Chapter I of this thesis are reproduced with permission from the article in Journal of Experimental Biology of which I am an author (Yoke and Shingyoji, 2017).

Materials and Methods

Preparation of 21S dynein and microtubules

21S dynein was prepared from sperm flagella of the sea urchins *Pseudocentrotus depressus*, *Hemicentrotus pulcherrimus* and *Strongylocentrotus nudus*, according to procedures described previously (Yoshimura and Shingyoji, 1999; Imai and Shingyoji, 2003; Inoue and Shingyoji, 2007) with some modifications. Sperm suspended in Ca^{2+} -free artificial seawater (465 mmol l^{-1} NaCl, 10 mmol l^{-1} KCl, 25 mmol l^{-1} MgSO_4 , 25 mmol l^{-1} MgCl_2 and 2 mmol l^{-1} Tris-HCl; pH 8.0) was treated for about 1–2 min with demembrating solution [0.1% (w/v) Triton X-100, 150 mmol l^{-1} potassium acetate, 2 mmol l^{-1} MgSO_4 , 10 mmol l^{-1} Tris-HCl, 2 mmol l^{-1} EGTA and 1 mmol l^{-1} dithiothreitol; pH 8.0] at room temperature. The demembrated sperm were resuspended in 150 mmol l^{-1} potassium acetate reactivating solution (150 mmol l^{-1} potassium acetate, 2 mmol l^{-1} MgSO_4 , 10 mmol l^{-1} Tris-HCl, 2 mmol l^{-1} EGTA and 1 mmol l^{-1} dithiothreitol; pH 8.0; without ATP) and were fragmented by passing through a 23-gauge hypodermic needle (Terumo, Tokyo, Japan) with a 1 ml syringe on ice. All the following procedures were performed on ice or at 4°C. After removal of the sperm heads by centrifugation at 2000 g, outer arm dynein was extracted from the axonemes by treatment with 0.6 mol l^{-1} NaCl (reactivating solution containing 0.6 mol l^{-1} NaCl instead of potassium acetate). The crude outer arm dynein was centrifuged on a 5–20% sucrose density gradient made in reactivating solution (containing 0.2 mol l^{-1} NaCl instead of potassium acetate) at 188,000 g for 12 h. The protein concentrations of the fractions were determined by the Bradford method (Bradford, 1976), using bovine serum albumin as a standard. The fractions with the highest protein concentrations were

adopted as purified outer arm dynein (21S dynein). 21S dynein in sucrose solution was kept in liquid nitrogen until use.

Tubulin was purified from porcine brains (Castoldi and Popov, 2003) by two cycles of polymerization-depolymerization in the presence of high molarity (final concentration: 0.5 mol l⁻¹) PIPES buffer, suspended in MES buffer (80 mmol l⁻¹ MES, 1 mmol l⁻¹ EGTA, 1 mmol l⁻¹ MgSO₄, 0.5 mmol l⁻¹ dithiothreitol) and stored in liquid nitrogen until use. Purified tubulin was labelled with tetramethylrhodamine (Hyman et al., 1991) using MES as a buffer and one cycle of polymerization-depolymerization instead of two. To obtain seeds, unlabelled tubulin and tetramethylrhodamine-labelled tubulin were mixed at a ratio of 5:1 and incubated at 33°C for 30 min in the presence of 5 mmol l⁻¹ GTP. The seeds were further polymerized by being mixed with unlabelled tubulin and tetramethylrhodamine-labelled tubulin at a ratio of 4:50:5 and incubated at 33°C for 20 min. Polymerized microtubules were stabilized by addition of 0.1 mmol l⁻¹ paclitaxel.

Observation of microtubule sliding, application of mechanical manipulation, and recording and analysis of response

For induction of microtubule sliding, the method of *in vitro* motility assay of dynein (Paschal et al., 1987; Vale and Toyoshima, 1988) was modified based on the method of the micromanipulation assay described previously (Morita and Shingyoji, 2004). By being diluted with 50 mmol l⁻¹ potassium acetate reactivating solution (50 mmol l⁻¹ potassium acetate, 2 mmol l⁻¹ EGTA, 2 mmol l⁻¹ MgSO₄, 1 mmol l⁻¹ dithiothreitol and 10 mmol l⁻¹ Tris-HCl; pH 8.0), 21S dynein at a concentration of 100–350 µg ml⁻¹ was obtained. Then 21S dynein (10 µl) was introduced into a 1.4 µl-perfusion chamber

constructed with two glass coverslips (24 mm×50 mm and 6 mm×18 mm) and 60 μm -thick mending tapes (Nichiban, Tokyo, Japan) used as a spacer. To induce microtubule sliding, microtubules (final concentration, 6 $\mu\text{g ml}^{-1}$) suspended in assay buffer containing ATP [20 mmol l^{-1} glucose, 216 $\mu\text{g ml}^{-1}$ glucose oxidase, 36 $\mu\text{g ml}^{-1}$ catalase, 1% (v/v) 2-mercaptoethanol, 10 $\mu\text{mol l}^{-1}$ paclitaxel and 1 mmol l^{-1} ATP, with or without ATP regeneration system in reactivating solution; 10 μl] were successively introduced into the chamber after the perfusion of 21S dynein. As the ATP regeneration system, 0.5 mg ml^{-1} creatine kinase and 5 mmol l^{-1} creatine phosphate were used.

To obtain an open surface over the sliding microtubules, which makes it possible to apply mechanical manipulation with a glass microneedle to the microtubules, 150 μl of assay buffer with 1 mmol l^{-1} ATP was added on the smaller (upper) coverslip, and the smaller coverslip was carefully slid sideways with tweezers (Fig. 1-1). Microtubules sliding on the glass surface at the bottom of the 150 μl pool of assay buffer were observed at room temperature (21–28°C) under an inverted fluorescence microscope (IX-70; Olympus, Tokyo, Japan) with a $\times 100$ oil-immersion objective lens (PlanApo; NA=1.4; Olympus), using a mercury arc lamp (USH-102D; Ushio, Tokyo, Japan) for excitation. The glass microneedles were made with a micropipette puller (PP-830; Narishige, Tokyo, Japan) and a glass rod (G-1000; Narishige). They were attached to and controlled by a water hydraulic micromanipulator (MW-3; Narishige), with the angle of approach to the coverslip around 20 deg. A glass microneedle was visualized simultaneously with the microtubules as a phase-contrast image using a halogen lamp for illumination. The movements of microtubules and glass microneedles were recorded with an image-intensified CCD camera (C2400-77; Hamamatsu Photonics, Hamamatsu, Shizuoka, Japan) and a hard disk drive recorder.

Movies were prepared by cropping the recorded data with NIH Image software (National Institutes of Health, Bethesda, MD, USA). Sequential images were prepared by capturing the movies with ImageJ (version 1.49h; National Institutes of Health). For calculation of the sliding velocities of microtubules, the sliding distances of the anterior or posterior end of the microtubules within a certain period of time (a few seconds) were measured either by ImageJ or by tracing the positions on to a transparent film fixed on a display. The time course of the position of microtubule ends were made with MTrackJ Plugin for ImageJ (Meijering et al., 2012). The tracings of the shapes of the microtubules were made using software for automatic tracking of a cilium along its length (Bohboh, BohbohSoft; Shiba et al., 2002).

Results

Microtubule sliding induced by dyneins in the open surface chamber

In the present *in vitro* motility assay using open surface chambers, microtubule sliding was induced by dynein molecules adsorbed onto a glass surface of a perfusion chamber. In a separate experiment using polarity-marked microtubules (Shingyoji et al., 1998, 2015), it was confirmed that the anterior end of a microtubule is always the plus end. In the present study, I tried to manipulate such microtubules moving on dyneins with a microneedle (Fig. 1-1). Like most of the studies using the *in vitro* motility assay, I used singlet microtubules polymerized from brain tubulin. There has been a report on using axonemal tubulin (95%)-derived microtubules for the *in vitro* motility assay of axonemal dynein, but it only shows higher velocity in short (<6 μm) conspecific microtubules than those polymerized from porcine brain tubulin (100%), and does not show any significant difference in longer microtubules (Alper et al., 2013; see the next section for the description of the lengths of the microtubules used in the present study). Micromanipulation was carried out according to the previously developed method (Morita and Shingyoji, 2004; Hayashi and Shingyoji, 2008) with some modifications. In the open-surface chamber of the present study, sliding velocity of the microtubules was $4.6 \pm 1.1 \mu\text{m s}^{-1}$ (mean \pm s.d. at 27°C; $N=15$, 150 $\mu\text{g ml}^{-1}$ dynein from *Pseudocentrotus depressus*), which is comparable to those shown in the conventional *in vitro* motility assay ($3.5 \pm 1.3 \mu\text{m s}^{-1}$; Paschal et al., 1987; and around 6 $\mu\text{m s}^{-1}$; Moss et al., 1992). As reported for the conventional *in vitro* motility assay (Paschal et al., 1987; Vale and Toyoshima, 1988), microtubules in the present assay system also showed unidirectional sliding towards their longitudinal axis, occasional spontaneous stoppage and

spontaneous recovery of sliding; of 367 sliding microtubules observed without manipulation in three separate experiments (by using $150 \mu\text{g ml}^{-1}$ 21S dynein obtained from *Pseudocentrotus depressus*), 79 (22%) microtubules showed spontaneous stoppage (once or more) during crossing the observation field ($87 \times 115 \mu\text{m}$). The average duration of the stoppage was 5.1 s ($N=66$) and its peak duration was 0–2 s. Microtubule sliding was observed for more than 20 min after perfusion with ATP, both in the presence and absence of ATP regeneration system.

Planar bending of sliding microtubules induces forward sliding and stoppage

Mechanical manipulation was applied to a sliding microtubule with a glass microneedle so as to bend a part of the microtubule in one plane. In other words, microtubules were bent within the plane parallel to the glass surface, thereby interesting responses including stoppage and backward sliding were induced. In a few cases when lower concentration ($100 \mu\text{g ml}^{-1}$) of dynein was used, micromanipulation provided bending in three-dimensional effects and dissociation of microtubules occurred. Details of the dissociation will be described later (see Results, Three-dimensional effects caused dissociation). Unless otherwise noted, responses induced by imposed bending were not affected by conditions, including the presence or absence of ATP regeneration system, different kinds of sea urchins for dynein and dynein concentrations used for motile assay.

Of 574 trials of planar bending applied to 260 sliding microtubules (length: $25 \pm 14 \mu\text{m}$, mean \pm s.d., ranging from 3 to $79 \mu\text{m}$, $N=574$), 434 trials (76%) resulted in continuation of forward sliding, as shown in Fig. 1-2A. An apparent decrease in sliding velocity was observed in 37 trials of the 434 (see the next section). I found that in 136

(23%) of the 574 trials, microtubules stopped sliding with imposed planar bending and stayed apparently stationary on the glass surface just after the microneedle was removed from the microtubule (Fig. 1-2B). In the remaining four cases under planar bending, I observed backward sliding (see below). The lengths of the microtubules that showed each of those responses (decrease in velocity, $21 \pm 9 \mu\text{m}$, $N=37$; stoppage, $26 \pm 14 \mu\text{m}$, $N=136$; backward sliding, $36 \pm 9 \mu\text{m}$, $N=4$; means \pm s.d.) were not significantly different from those ($25 \pm 14 \mu\text{m}$, $N=434$, mean \pm s.d.) of the microtubules with continuous forward sliding (Mann–Whitney U-test, $P>0.05$).

When planar bending was applied to a sliding microtubule with a glass microneedle, in addition to the shape change of the microtubule induced by the movement of the glass microneedle (0–0.8 s in Fig. 1-2A), changes in mechanical state between the dynein–microtubule interactions on the glass surface would be induced. Here, I consider three categories of strain imposed on dyneins to be important. One is the lateral strain, which shifts a microtubule laterally from the original position ('a' in the bottom panel of Fig. 1-2A). This strain is mainly imposed on a microtubule at the region of contact with the glass microneedle. Secondly, microtubules and dyneins experience pulling strain along the length of a microtubule towards the point of contact with the glass microneedle ('b' in the bottom panel of Fig. 1-2A). This strain results from the tension of the microtubule. Thirdly, elastic strain resulting from bends of a microtubule is imposed on dyneins ('c' in the bottom panel of Fig. 1-2A). This kind of strain works in a direction so as to decrease the curvature of the bend of the microtubule. The first one (lateral strain, a) and the second one (pulling strain, b) are active only during imposed bending of a microtubule with moving the glass microneedle, whereas the third one (elastic strain, c) is always active as long as the bend of the microtubule is

present and independent of the glass microneedle and its movement.

Decrease in sliding velocity induced by planar bending

Of 434 cases showing continuation of forward sliding by planar bending, 37 brought about apparent decrease in sliding velocity. One example is shown in Fig. 1-3A. I measured a change of the sliding path distance within 3.2 s of the stable phase before, during and after imposed bending and obtained the sliding velocities. The time-dependent change in the path distance (absolute value) of the anterior end of the same microtubule as shown in Fig. 1-3A is analysed in Fig. 1-3B. The slope of this plot, representing the sliding velocity, decreased during bending. In Fig. 1-3C the average sliding velocities in three states, before bending, during bending and after the bend dissolved, are plotted for nine cases. The average sliding velocities were low during bending while they were similarly high both before and after bending. In the state of ‘after the bend dissolved’ the microtubule bent with a microneedle became nearly straight after being released from imposed bending. The relationship between the percentage of decrease in the average sliding velocities, calculated from the rate before and during bending of each of the nine examples, and the bend angle were examined (Fig. 1-3D). The average sliding velocities were decreased by 28–93% in response to imposed bending of 44–221 deg. However, there was no statistical significance in fitting the linear regression model to the relationship between the percentage of decrease in the average sliding velocities (a dependent variable) and the bend angles (an independent variable) (F-test for linear regression analysis, $P>0.4$, $N=9$). These results suggest that imposed bending is able to decrease the sliding velocity, but the extent of decrease is not solely determined by the bend angles.

Stoppage of sliding was reversible

Stoppage of sliding microtubules induced by planar bending did not always recover sliding after removal of the microneedle. Of the 136 trials of planar bending that induced stoppage, about half (53%) recovered sliding spontaneously (i.e. without any further mechanical manipulations) (Fig. 1-4, filled box). In the remaining stoppage of 53 cases (Fig. 1-4, grey and hatched boxes), when planar bending was further applied, 34 of them recovered sliding (Fig. 1-4, grey box). Thus 78% (106 out of 136) of the microtubules that showed stoppage in response to the first imposed bending showed recovery of sliding (Fig. 1-4, filled and grey boxes). Some of the microtubules showing stoppage (19 out of 53 cases) were exposed to irreversible damage of severing a microtubule into two parts by the second manipulation (Fig. 1-4, hatched box). However, most of the 19 severed microtubules showed active behaviour: in 11 severed microtubules either half of the severed microtubules moved, and in six severed microtubules both parts of the severed microtubules moved.

Fig. 1-5A shows a typical example of the stoppage induced by imposed bending, accompanied by forward sliding due to spontaneous recovery. The microtubule was bent in the middle region with backward pulling of the anterior region, thereby stoppage occurred only in the anterior region (at 2.7–11.4 s), but after stoppage (for 8.7 s) the anterior region recovered sliding at 11.4 s and the whole length began to move (arrows). The distribution of duration of the stoppage for 34 cases is shown in Fig. 1-5B. The average duration was 9.6 s. These results indicate that stoppage induced by imposed bending was not the result of irreversible damage to dynein, but reflects a reversible state of stable dynein–microtubule crossbridges.

Conditions required for induction of stoppage

What kind of mechanical signals cause stoppage? From the observation of the microtubules that showed stoppage, I noticed that the anterior region (or the leading part) of the microtubule was often pulled backwards along with imposed bending, just before the stoppage of sliding. This suggests a possibility that backward-pulling strain caused by the movement of the microneedle (pulling strain, b in the bottom panel of Fig. 1-2A) may be important in inducing stoppage. To confirm this, I categorized the trials of planar bending according to the regions of bending and the presence/absence of backward displacement of the anterior region, and quantified the relative frequency of stoppage to the number of the trials of bending of each category. The relative frequency of stoppage to the number of trials of bending on the middle region of microtubules was significantly higher than that of bending on the posterior region ($P < 0.03$, chi-squared test; Fig. 1-6A), and the relative frequency of stoppage to the number of trials of bending on the middle region with a backward displacement of the anterior region was significantly higher than that without one ($P = 1 \times 10^{-5} < 0.01$, chi-squared test; Fig. 1-6B). This result suggests that backward pulling strain may be important for the induction of stoppage of sliding.

To further test the importance of backward strain on induction of stoppage, short ($9 \pm 4 \mu\text{m}$, mean \pm s.d.; ranging from 5 to 14 μm , $N=10$) sliding microtubules were pushed backwards by causing a head-on collision with a glass microneedle without bending. This kind of mechanical manipulation was technically difficult, but I have succeeded in doing so in 10 trials on seven sliding microtubules. While seven trials induced continuation of forward sliding, three trials of backward pushing induced stoppage. One example of those three trials is shown in Fig. 1-6C. This suggests that the

backward strain, not bending of microtubules itself, is important for induction of stoppage.

In 10 trials out of the 136 trials of bending that induced stoppage, only the anterior part of the microtubules became stationary while the posterior part (distal region) continued sliding at least for a period of time. In Fig. 1-6D imposed bending started at 0 s and the anterior region stopped sliding at 5.7 s (indicated in red in Fig. 1-6D), while the posterior region continued sliding (indicated in blue in Fig. 1-6D) between 5.7 and 14.4 s. I focused on the motion of the anterior part of this microtubule just before the stoppage of the anterior region, and found that the anterior part of the microtubule was pulled backwards (5.2–5.7 s) by the pulling strain caused by the glass microneedle (pulling strain, b in the bottom panel of Fig. 1-2A). Fig. 1-6E shows the superimposed tracings of the positions of the microtubule before and after backward pulling of the anterior region (at 5.2 and 5.7 s in Fig. 1-6D). The anterior end of the microtubule, indicated by the arrows, moved 1.0 μm backwards in 0.5 s. In all of the 10 cases where microtubules showed stoppage only in the anterior region (lengths of the microtubules: $42 \pm 15 \mu\text{m}$, mean \pm s.d., $N=10$), the anterior part was pulled backwards by the glass microneedle just before the stoppage of the anterior region. The distances of the backward displacement of the anterior end were 1.5 μm on average, and ranged from 0.3 to 3.3 μm ($N=10$). Stoppage only in the anterior region of a microtubule was never observed in microtubules that were not mechanically manipulated ($N=724$ microtubules). This further suggests the importance of backward strain in induction of stoppage of sliding.

Dynein concentration positively affected the frequency of occurrence of stoppage, while the presence of an ATP regeneration system or the species of sea

urchins used for preparation of dynein did not. In the experiments using $100 \mu\text{g ml}^{-1}$ 21S dynein, microtubules often slid with their one end dissociated and swaying, while in the experiments using more than $150 \mu\text{g ml}^{-1}$ 21S dynein almost all the microtubules slid with the whole length within the plane of focus. The results suggest that higher concentrations of perfused dynein, which probably lead to higher densities of dynein molecules on the glass surface, may result in higher affinity between dynein and microtubules, facilitating the conduction of strain from the manipulated microtubules to interacting dynein, causing the stoppage of sliding more frequently induced by mechanical manipulation.

When ATP in the perfusion chamber was almost consumed by ATPase activity of dynein, microtubules stopped sliding and became stationary on the glass surface, as reported previously for the *in vitro* motility assay without wash of excess dynein (Paschal et al., 1987). When excess amount of 21S dynein was removed with buffer solution before perfusion of ATP and microtubules, microtubules showed diffusive motion and dissociated from dynein after the exhaustion of ATP, which is consistent with the previous report for the conventional *in vitro* motility assay with wash of excess dynein (Moss et al., 1992). I confirmed that under the condition with wash of excess dynein, imposed bending can also induce stoppage of microtubule sliding. This suggests that stoppage can be induced by backward strain in an independent mechanism from the stationary state observed after ATP exhaustion and that the stoppage induced by mechanical manipulation is the result of reversible changes in modes of motility of active dynein molecules.

Backward sliding induced by continuous backward strain

Four out of the 574 trials of planar bending brought about a reversal in the sliding direction, which was never observed without mechanical manipulation. Four cases are few, but seem to represent a very important characteristic of dynein.

In three of the cases, backward sliding was induced only in the anterior region of the microtubules by bending the posterior region of the microtubules. One example is shown in Fig. 1-7A. This microtubule was sliding towards the lower left in the panel in Fig. 1-7A before bending (from -5.0 to 0 s). However, the anterior region changed the sliding direction towards the upper right when bending was applied in the posterior region. After bending, the glass microneedle was kept in the same position (indicated by an arrowhead, at 0.7 – 13.7 s in Fig. 1-7A). Superimposed tracings of the microtubules in Fig. 1-7A are shown in Fig. 1-7B. The anterior end of this microtubule moved $5.0\ \mu\text{m}$ towards the upper right, the opposite direction of original sliding, indicating the backward sliding along the anterior region of the microtubule. The position of the glass microneedle for bending was kept almost stable during the backward sliding, resulting in an increase in curvature of the bent region in Fig. 1-7A and B. The tip of the microneedle shifted a slight distance of about $0.6\ \mu\text{m}$ towards the lower direction between 0.7 and 13.7 s, possibly due to pushing force of the backward sliding in the anterior region of the microtubule. The backward sliding for a few seconds was accompanied by dissociation and displacement of the anterior region of the microtubule at 18.8 s, which then is followed by recovery of the slow forward sliding at 34.5 s. Slow forward sliding recovered the original velocity after sliding microtubule released from bending constriction with the microneedle at 46.1 s. These results show that the backward sliding is not the result of passive movement caused by the movement of the

glass microneedle, but is driven by sliding induced by dynein motors.

What kind of signal is important for inducing backward sliding? In all of the three cases where backward sliding was induced only in the anterior region of the microtubules, bend angles were more than 140 deg (1–3 in Table 1-1), and the glass microneedle was kept stationary at the place of imposed bending, which resulted in keeping the bent region of the microtubules during the backward sliding. In such a condition, elastic strain of the microtubule (c in the bottom panel in Fig. 1-2A) must be imposed on the anterior region of the microtubule continuously. Elastic strain works in the direction such that it decreases the curvature of the microtubule, so the anterior region of the microtubule and the interacting dynein are estimated to receive elastic strain in an angled backward direction. These suggest that continuous backward strain may be important for inducing backward sliding.

In the remaining case among the four, backward sliding was induced in the whole length of the microtubule (Fig. 1-7C). The microtubule sliding towards the lower right (at -6.5 to 0 s) was bent in the posterior region and the glass microneedle was kept attached to the microtubule (indicated with arrowheads at 1.9–74.9 s). Both the anterior end and the posterior end of the microtubule moved backward, in the opposite direction of the original sliding (1.9–74.9 s). Superimposed tracings of this microtubule show that the whole length of the microtubule translocated almost along a single track during the backward sliding (Fig. 1-7D). This microtubule recovered forward sliding after the backward sliding (74.9–87.9 s), and proceeded on the same track as the previous backward sliding (the dotted line in Fig. 1-7D). This result suggests that backward sliding can be induced as a result of reversible change in sliding direction of a single set of dynein molecules interacting with the microtubule.

In this case, the glass microneedle was slowly shifted towards the bottom of the image for 3.0 μm while the microtubule slid backward for 2.3 μm (1.9–74.9 s in Fig. 1-7C, number 4 in Table 1-1). Considering the steric geometry of the microtubule and the glass microneedle, where the tip of the glass microneedle was obliquely attached to the glass surface and the microtubule was located between the microneedle and the glass surface, the posterior region of the microtubule might have been pulled backwards by the motion of the microneedle. Together with the analyses of the three microtubules that showed backward sliding only in the anterior region, this result suggests that continuous backward strain may be important in inducing backward sliding.

Although there was no statistically significant difference ($P>0.05$, randomized test on matched samples), the velocities of the backward sliding shown during bending tended to be smaller than the forward sliding velocities before bending (Table 1-1). This does not appear characteristic of backward sliding because the velocities of the forward sliding following the backward sliding (exerted before the bend dissolved) also tended to be slower than that exerted after the bend dissolved. These suggest that imposed bending may induce decrease in sliding velocity in both forward and backward sliding, possibly through a common mechanism such as continuous elastic strain resulting from the bend of the microtubules.

Three-dimensional effects caused dissociation

Ten trials of imposed bending with a three-dimensional effect, in which microtubules were bent in a three-dimensional way, not within the plane parallel to the glass surface, induced dissociation of the microtubules. In two of these cases the dissociation occurred only in a short period; the glass microneedle was inserted between a microtubule and

the glass surface, thus a part of the microtubule transiently dissociated from dynein on the glass surface, with the rest of the microtubule continuing to slide on the glass surface, then eventually the whole length came back to the plane of focus and recovered forward sliding. In the other eight cases, the whole length of the microtubule dissociated from dynein on the glass surface (complete dissociation). In one of these eight cases, the middle region of a microtubule was pushed down towards the glass surface by the glass microneedle and the microtubule was bent so that the anterior and posterior region dissociated from dynein on the glass surface, followed by dissociation of the whole length. In the other seven cases, the glass microneedle was inserted and moved between a microtubule and the glass surface, causing dissociation of the whole length of the microtubule (Fig. 1-8). The relative frequency of dissociation to the number of mechanical manipulations was significantly higher when the concentration of perfused dynein was $100 \mu\text{g ml}^{-1}$ than when it was 150 or 180–200 $\mu\text{g ml}^{-1}$, probably because the microneedle was more easily inserted between the microtubule and the glass surface when the dynein density was lower, due to the lower affinity between dyneins and microtubules. These results suggest that adequate strain, which is perpendicular to the glass surface, can induce dissociation of microtubules from dynein.

Discussion

In the present study, to understand the behaviour of an ensemble of dynein molecules under mechanical signals, the microtubule sliding induced by outer arm dynein was investigated. I found that planar bending can induce three different modes of motility of dynein: continuation of forward sliding, stoppage of sliding and backward sliding. Decrease in sliding velocity was also induced by planar bending. For induction of the stoppage and backward sliding, the importance of backward strain is suggested. Moreover, imposed bending with a three-dimensional effect induced dissociation of the microtubules from dyneins. While this is a novel *in vitro* experimental system to investigate the mechanical properties of dynein, we should also pay attention to the limitation of the present experimental set-up, in which dyneins interact with singlet microtubules and a glass surface, unlike the intact situation with the doublet microtubules.

Induction of a stationary mode of dynein

Stoppage (stationary mode) induced in the present study was distinct from dissociation. The microtubules that showed stoppage remained within the plane of focus without diffusive motion, implicating the sustained interaction with dynein (Fig. 1-2B), whereas dissociated microtubules went out of focus and showed diffusive motion (Fig. 1-8). Based on the cyclical response consisting of bending, pause with a constant curvature and dissociation observed in a pair of doublet microtubules of a frayed flagellar axoneme, dyneins are thought to change their modes from sliding to stationary in response to external strain without detachment from the microtubule at a low

concentration ($10 \mu\text{mol l}^{-1}$) of ATP (Lindemann, 2014; Mukudan et al., 2014). Stoppage of sliding in the present study suggests that this is also the case even at a high, physiological concentration (1mmol l^{-1}) of ATP. Furthermore, in addition to transverse strain (t-force; Lindemann and Lesich, 2015), the present study indicates that backward, parallel strain may also be important in inducing stoppage of sliding.

It appears that there is a natural fluctuation between the forward sliding mode and the stationary mode of dynein molecules, because 53% (72 out of 136) of the microtubules that showed stoppage in response to mechanical manipulation recovered sliding spontaneously in several seconds (Figs 1-4 and 1-5A,B). Microtubules that were not manipulated with the glass microneedle also showed occasional transient stoppage and recovery of sliding (see Results, Microtubule sliding induced by dyneins in the open surface chamber). Transient stoppage and recovery of sliding of microtubules were also reported in the study of conventional *in vitro* motility assay of dynein (Vale and Toyoshima, 1988). If this occasional stoppage and recovery is the result of fluctuation of modes of motility of individual dynein molecules, the role of external strain may be coordinating the activities of a set of dynein molecules along a microtubule simultaneously to a stationary mode.

Bidirectionality

Early studies on sliding disintegration of axonemes (Sale and Satir, 1977; Fox and Sale, 1987) or studies on *in vitro* motility assay (Paschal et al., 1987; Vale and Toyoshima, 1988) reported only unidirectional motility induced by dynein. However, ATP-dependent bidirectional stepping of dynein (Shingyoji et al., 1998) and bidirectional force generation by dynein (Shingyoji et al., 2015) under strain imposed by

an optical trap has been reported in single molecule (or two to four molecule) analyses, and bidirectional stepping of a single cytoplasmic dynein molecule under strain imposed by an optical trap has also been reported (Gennerich et al., 2007). Although backward sliding was induced only in rare cases (four cases out of 574 trials of planar bending) in the present study, they suggest that ensemble of dynein molecules can collectively support backward sliding of microtubules in response to external strain, either by strain-dependent backward stepping of dyneins or by backward force generation by dyneins. Backward strain was suggested to be important for induction of backward sliding in the present study, and this direction is consistent with the previous reports on single molecule analyses (Gennerich et al., 2007; Shingyoji et al., 2015). In the present study, dyneins adsorbed onto the glass surface are supposed to be oriented in every direction, and I cannot preclude a possibility that some dyneins are attached to a microtubule in the wrong direction and that such dyneins may be involved in the backward sliding. However, the induction of backward sliding in microtubules interacted with dyneins arrayed on doublet microtubules (Shingyoji et al., 2015; Shingyoji, 2017) indicates that uniformly oriented dyneins are also capable of backward sliding. A possible interpretation of this finding in the context of beating axonemes is discussed below.

Decrease in sliding velocity

Decrease in sliding velocity was induced while the bend was formed, and the velocity recovered after the bend dissolved (Fig. 1-3). This suggests that an ensemble of outer arm dynein molecules can not only be switched between on/off or stop/go, but can modify collective sliding velocity in a reversible manner in response to a mechanical

signal in the presence of a high concentration (1 mmol l^{-1}) of ATP. It is not yet clear whether the curvature of microtubules is important, or if some kind of external strain is important for the induction of velocity change, but considering the previous reports that decrease in sliding velocity of a single axonemal and cytoplasmic dynein molecule can be induced by backward strain imposed by an optical trap (Hirakawa et al., 2000; Rai et al., 2013), backward strain resulting from the elasticity of bent microtubules may be important for induction of decrease in sliding velocity in the present study.

Strain-dependent regulation of outer arm dynein in an axoneme

The roles of outer arm dynein and inner arm dynein in the axonemes have been suggested to be somewhat different. While flagella of inner arm-deficient mutants of *Chlamydomonas reinhardtii* showed a reduction in shear amplitude with only a small reduction in beat frequency, those of outer arm-deficient mutants showed beating with a reduced frequency to about half that of wild-type flagella (Brokaw and Kamiya, 1987). Also, sea urchin sperm flagella that were extracted with demembrating detergent along with 0.5 mol l^{-1} KCl to remove outer arm dynein could be reactivated with ATP to produce bending waves whose wave forms are not significantly different from normal, but have a reduced beat frequency of about half that of control demembrated sperm without exposition to 0.5 mol l^{-1} KCl (Gibbons and Gibbons, 1973). These suggest that the primary function of outer arm dynein is increasing propagation velocity (Brokaw, 1994, 1999) by mainly contributing to the metachronal sliding, exerting a maximum shear force and sliding at the bend regions of an axoneme, and decreasing sliding velocity to nearly zero on the straight regions, where the reversal of the inter-doublet sliding direction occurs (Brokaw and Gibbons, 1975; Gibbons, 1981) (see upper panel

in Fig. 1-9A). In the present study, stoppage and backward sliding of purified outer arm dynein on a glass surface were induced by backward strain (Fig. 1-9B). This might reflect the regulatory mechanism of the sliding activities (such as sliding velocities and directionalities) of outer arm dynein in a beating axoneme, which could be regulated and coordinated by backward strain imposed on dynein at straight regions as elastic resistance (Fig. 1-9A) (Brokaw, 2001).

This strain-dependent regulatory mechanism alone may not be sufficient to explain the whole picture of flagellar movement. For example, in asymmetrically beating flagella, synchronous sliding occurs throughout the region distal to the proximal principal bend (Goldstein, 1977). The synchronous sliding that accompanies the growth of the proximal principal bend seems to impose shear strain on dyneins in the distal regions, but it does not apparently affect the propagation of the pre-existing bends (Goldstein, 1977). It is likely that the dyneins are capable of integrating various components of information, which include shear strain, as well as transverse force that accompanies the curvature of an axoneme (Lindemann, 1994a,b; Lindemann and Lesich, 2015), and signals related to calcium ion (Brokaw, 1979). The present result suggests that isolated outer arm dyneins have the ability to respond to mechanical signals of strain, which might reflect an important aspect of the communication within a beating axoneme and a basic requirement for the overall flagellar oscillation. I hope that the present experimental system provides a basis for more detailed, quantitative approach for understanding the mechanical properties of dynein in the future.

Table 1-1

Parameters concerning to the backward sliding induced by imposed bending.

Number	Bend angle (deg)	Distance of the backward sliding (μm)	Forward sliding velocity before bending ($\mu\text{m s}^{-1}$)	Velocity of the backward sliding ($\mu\text{m s}^{-1}$)	Velocity of the forward sliding following the backward sliding ($\mu\text{m s}^{-1}$)	Forward sliding velocity after the bend dissolved ($\mu\text{m s}^{-1}$)	Related figures
1	140	5.0	2.1	0.64	0.34	1.3	Fig. 1-7A
2	194	1.0	1.4	0.53	0.54	0.81	—
3	161	1.2	4.4	0.90	0.67	3.6	—
4	159	2.3	2.8	0.060	0.67	2.8	Fig. 1-7C

For each of the 4 microtubules (numbers 1–4) that showed backward sliding by imposed planar bending, imposed bend angles, sliding distances and sliding velocities are shown. Bend angles at the beginning of the backward sliding are shown. See inset of Fig. 1-3D for the definition of a bend angle.

Fig. 1-1

Schematic depiction of the experimental setup. Microtubule sliding was induced by consecutive perfusion of 21S dynein and then of microtubules with 1 mmol l^{-1} ATP to the perfusion chamber (top panel). Following the perfusion, the upper coverslip of the perfusion chamber was slid sideways (thick arrow) with a tweezer to obtain an open surface, which enabled the micromanipulation of the sliding microtubules with a glass microneedle.

Fig. 1-1

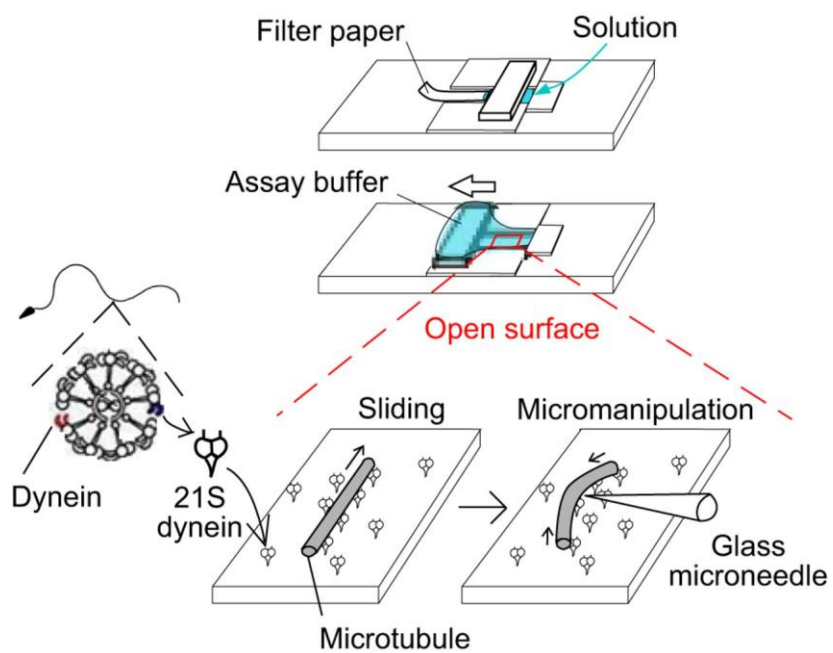


Fig. 1-2

Planar bending induced continuation of forward sliding and stoppage of sliding.

(A) Sequential images taken from the original data of a microtubule (MT) showing continuation of forward (Fw) sliding after imposed planar bending. The numbers in the upper left corner of each panel are time (s) counted after the bending started, and the sliding direction of a microtubule is indicated by the arrows. The position of the tip of a glass microneedle used for bending is indicated by arrowheads in the panels in which bending was performed. The microtubule moved from the upper right corner to the left, and changed the moving track slightly downwards after imposed bending (0.8 s and thereafter). The bottom panel shows the superimposed tracings of the microtubule before (interrupted line) and after (blue continuous line) imposed bending (0 and 0.8 s), and red arrows indicate three kinds of external strain that are estimated to be imposed on the microtubule and dyneins with planar bending: lateral strain (a), pulling strain (b) and elastic strain (c). Scale bars, 10 μm . (B) Sequential images of a microtubule showing stoppage of microtubule sliding induced by planar bending. This microtubule moving towards the upper left direction showed stoppage when the posterior region was bent (0.6–0.9 s, and the bottom illustration), and became stationary (0.9–10.5 s). The arrowhead marks the position of the tip of the glass microneedle at 0.6 s. Scale bar, 10 μm .

Fig. 1-2

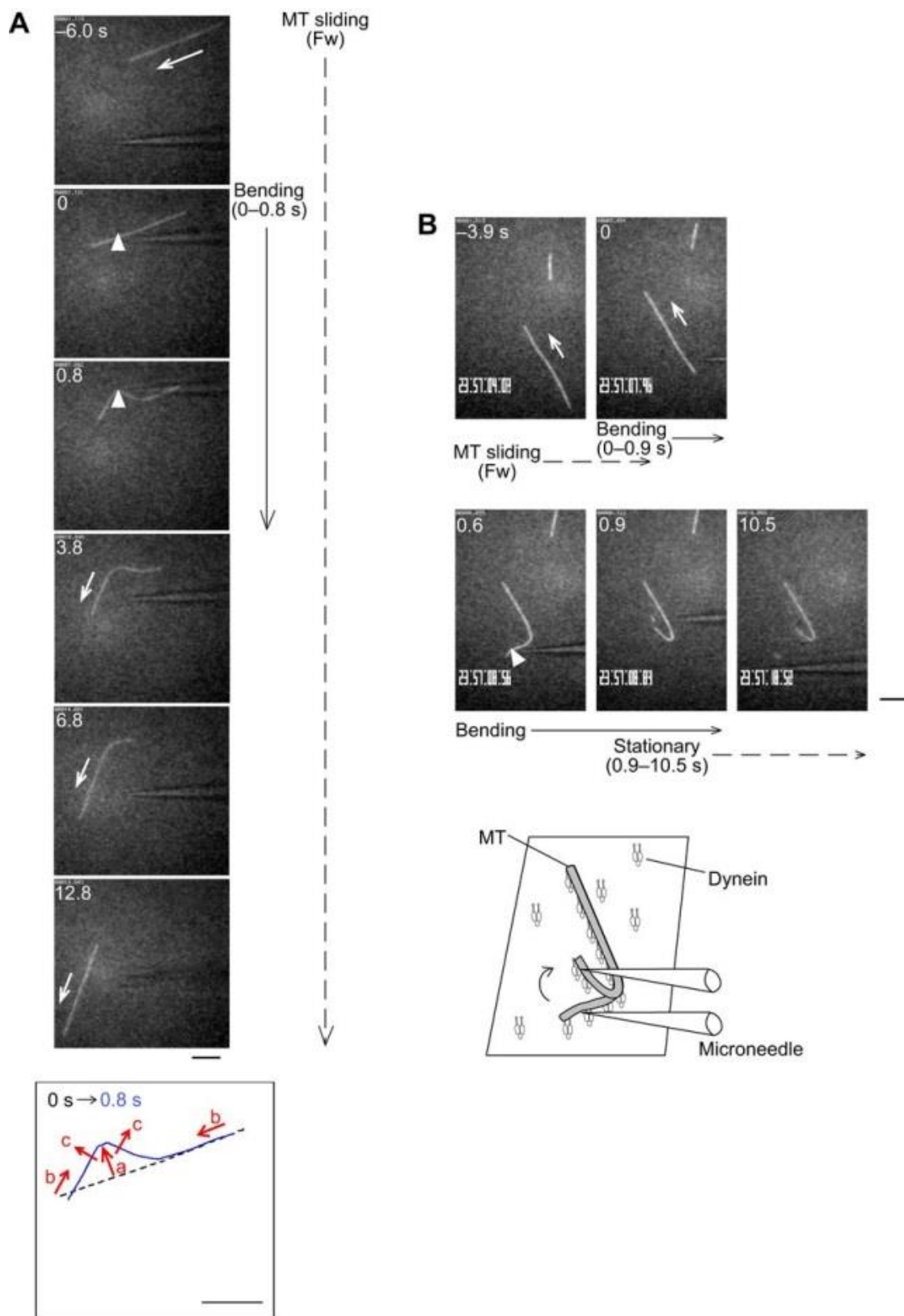


Fig. 1-3

Decrease in sliding velocity induced by planar bending. (A) Sequential images of a microtubule (indicated with blue) that showed decrease in sliding velocity in response to planar bending. Two sequential images with an interval of 3.2 s, which was used for measuring displacement (path distance), are shown for each of the three bending states: before, during and after bending. The arrows show the anterior end of the microtubule. Fw, forward sliding. Scale bar, 10 μm . (B) The time course of the change in path distance of the anterior end of the same microtubule shown in A. The sliding velocity, which is equivalent to the slope of this plot, was decreased during bending, and recovered after bending. The arrowheads represent examples of passive motions of the anterior end caused by movements of the glass microneedle during bending of the microtubule. The periods shown by the asterisks were used for calculation of average sliding velocities plotted in C. (C) The average sliding velocities before bending, during bending, and after the bend dissolved, are plotted for nine microtubules. They showed decrease in velocity by bending. Each set of three dots connected by a continuous line indicates data from a single microtubule, and the open circles indicate the data from the microtubule shown in A and B. (D) The percentages of decrease in average sliding velocities, calculated from the average sliding velocities before bending and during bending, are plotted against the bend angles (θ) for the nine microtubules (MT). The definition of the bend angle θ is shown in the inset. Each filled circle represents a datum from a single microtubule and the open circle represents the datum from the microtubule shown in A and B.

Fig. 1-3

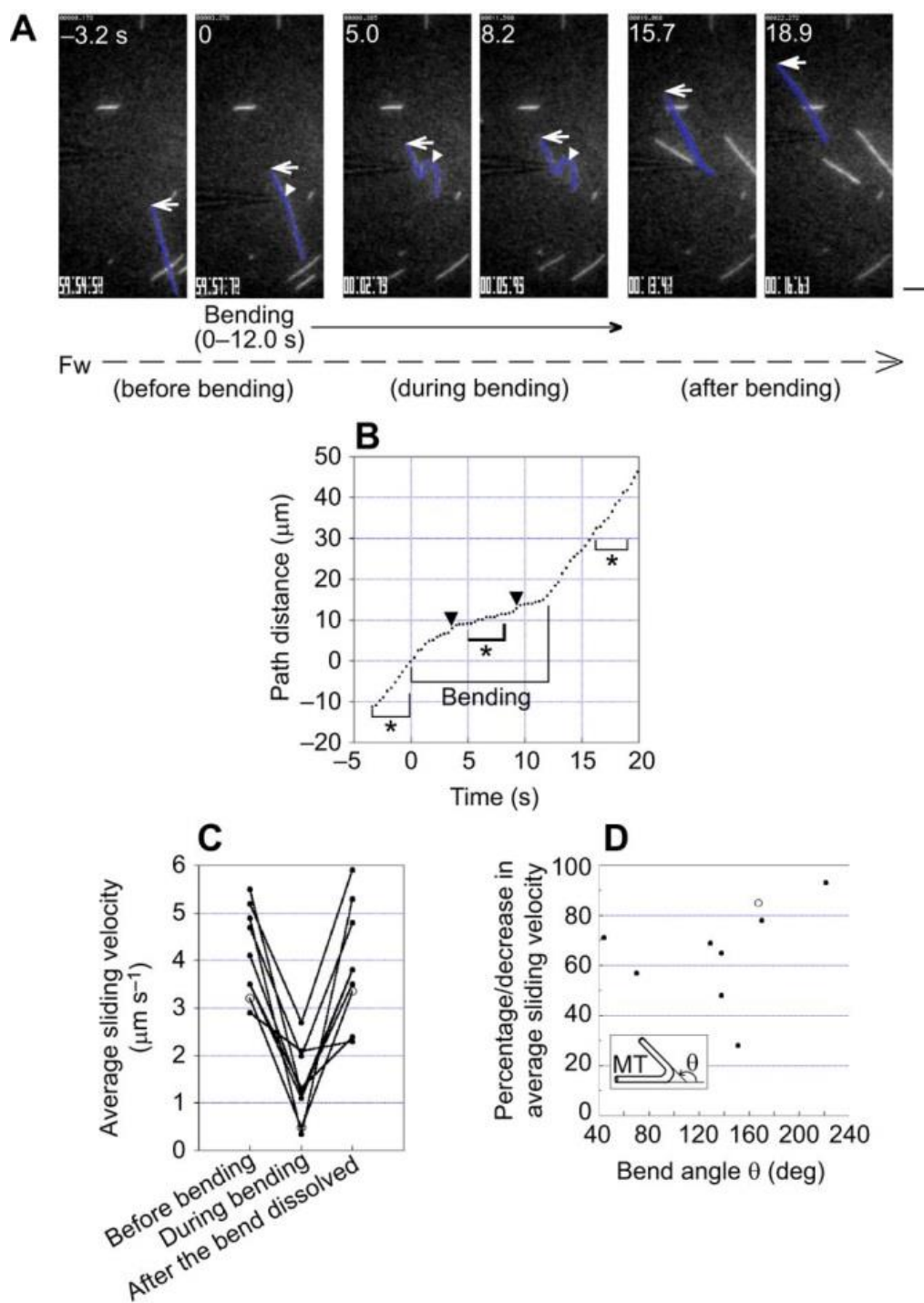


Fig. 1-4

Behaviour of the microtubules that showed stoppage by planar bending of the first manipulation. Most of the microtubules ($N=106/136$) that became stationary by planar bending recovered sliding movement spontaneously (filled box) or by the second bending (grey box). The relative frequency of recovery of sliding to the number of bending-induced stoppage was approximately 80%. Remaining cases were microtubule severing (hatched box) and no further response (open box). N , number of trials of imposed bending.

Fig. 1-4

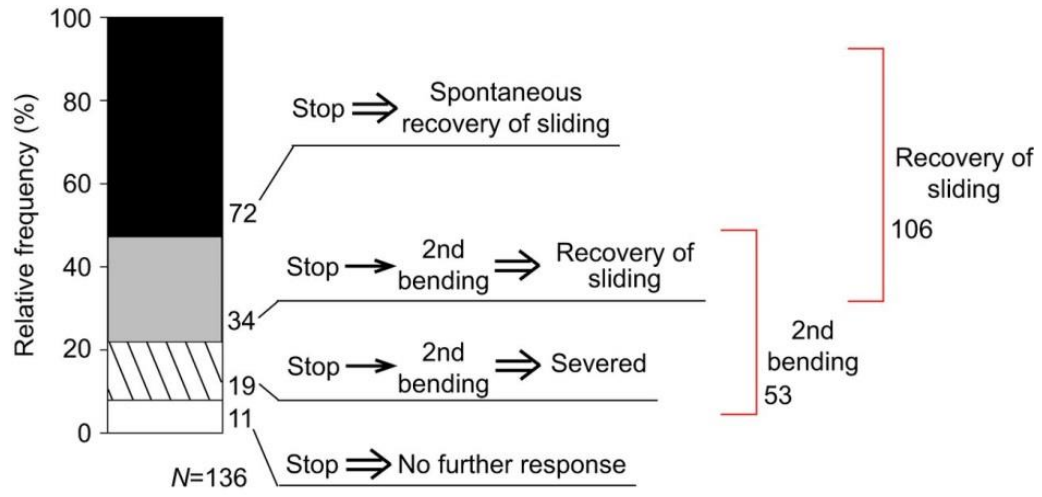


Fig. 1-5

Recovery of sliding in microtubules that showed stoppage. (A) Sequential images of a microtubule that showed spontaneous recovery of sliding after stoppage. The anterior region, which stopped sliding in response to planar bending and became stationary between 2.7 and 11.4 s, recovered sliding at 11.4 s. Fw, forward sliding. Scale bar, 10 μm . (B) Distribution of the durations of stoppage induced by mechanical manipulation. The data are from the experiments with $150 \mu\text{g ml}^{-1}$ 21S dynein from sperm of *Pseudocentrotus depressus* in assay buffer with an ATP regeneration system. N , number of microtubules.

Fig. 1-5

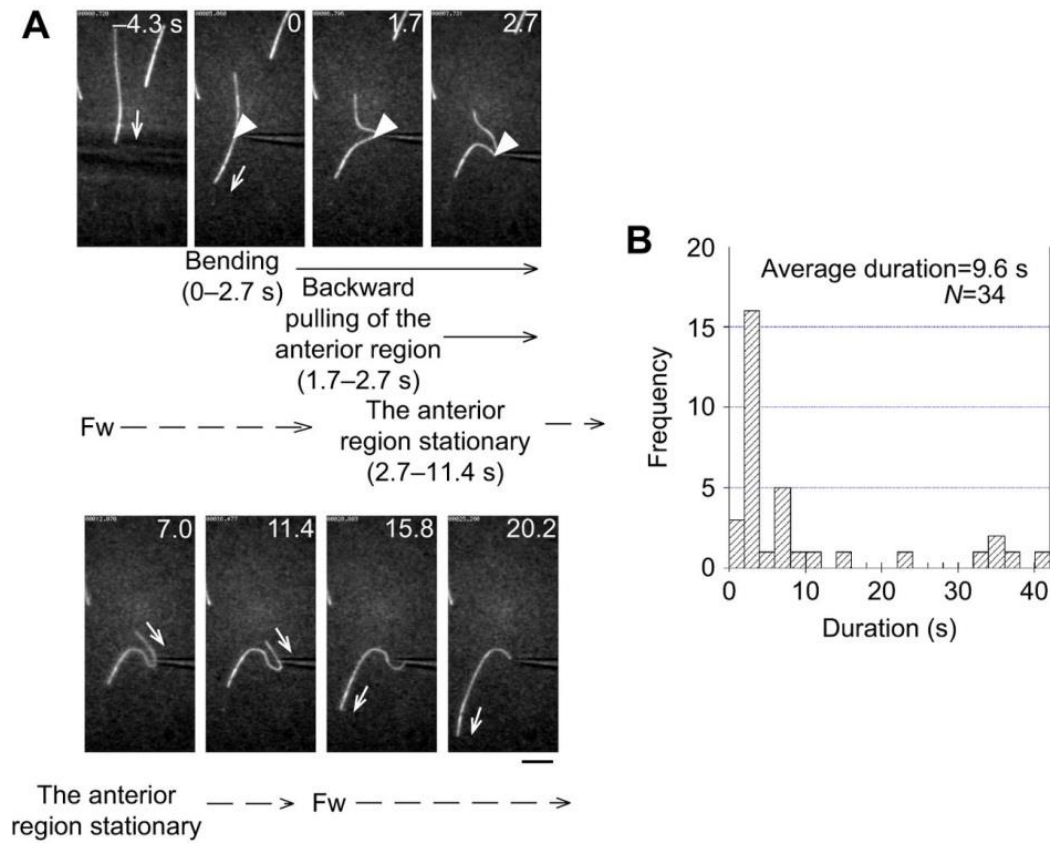


Fig. 1-6

Backward strain is important for induction of stoppage. (A) Effect of regional difference of bending on the relative frequency of occurrence of stoppage; data from the experiments using $150 \mu\text{g ml}^{-1}$ 21S dynein obtained from *Pseudocentrotus depressus* and assay buffer with an ATP regeneration system are shown. N , number of manipulations; $*P < 0.03$, chi-squared test. (B) Effect of the backward displacement of the anterior region on the relative frequency of occurrence of stoppage; data from the experiments using $150 \mu\text{g ml}^{-1}$ 21S dynein obtained from *Pseudocentrotus depressus* and assay buffer with an ATP regeneration system are shown. $**P = 1 \times 10^{-5} < 0.01$, chi-squared test. (C) Backward pushing without bending also induced stoppage. Sequential images of a microtubule that showed stoppage in response to backward pushing without bending are shown. The numbers in the upper left corner of each image indicate the time (seconds) after the beginning of backward pushing. The sliding microtubule (-4.6 to 0 s) was pushed backwards, causing head-on collision with the glass microneedle at $0-0.4$ s, and became stationary ($0.4-30.4$ s). The positions of the anterior end of the microtubule before and after backward pushing are indicated by open and filled arrowheads, respectively. Fw, forward sliding. Scale bar, $10 \mu\text{m}$. (D) Sequential images of a microtubule that showed stoppage in the anterior region in response to imposed bending. The microtubule was bent in the middle region ($0-5.7$ s) and only the anterior region of the microtubule showed stoppage, while the rest continued forward sliding ($5.7-14.4$ s). A sliding region and a stationary region of the microtubule are indicated in blue and red (at 5.7 and 10.1 s), respectively. Just before the stoppage of the anterior region, the anterior region was pulled backwards by the glass microneedle ($5.2-5.7$ s). Scale bar, $10 \mu\text{m}$. (E) Diagram showing superimposed tracings of the same microtubule in D before and after the backward pulling of the anterior region. The blue dotted line indicates the microtubule at 5.2 s, and the blue and red continuous lines indicate the regions of the microtubule sliding and being stationary at 5.7 s.

Fig. 1-6

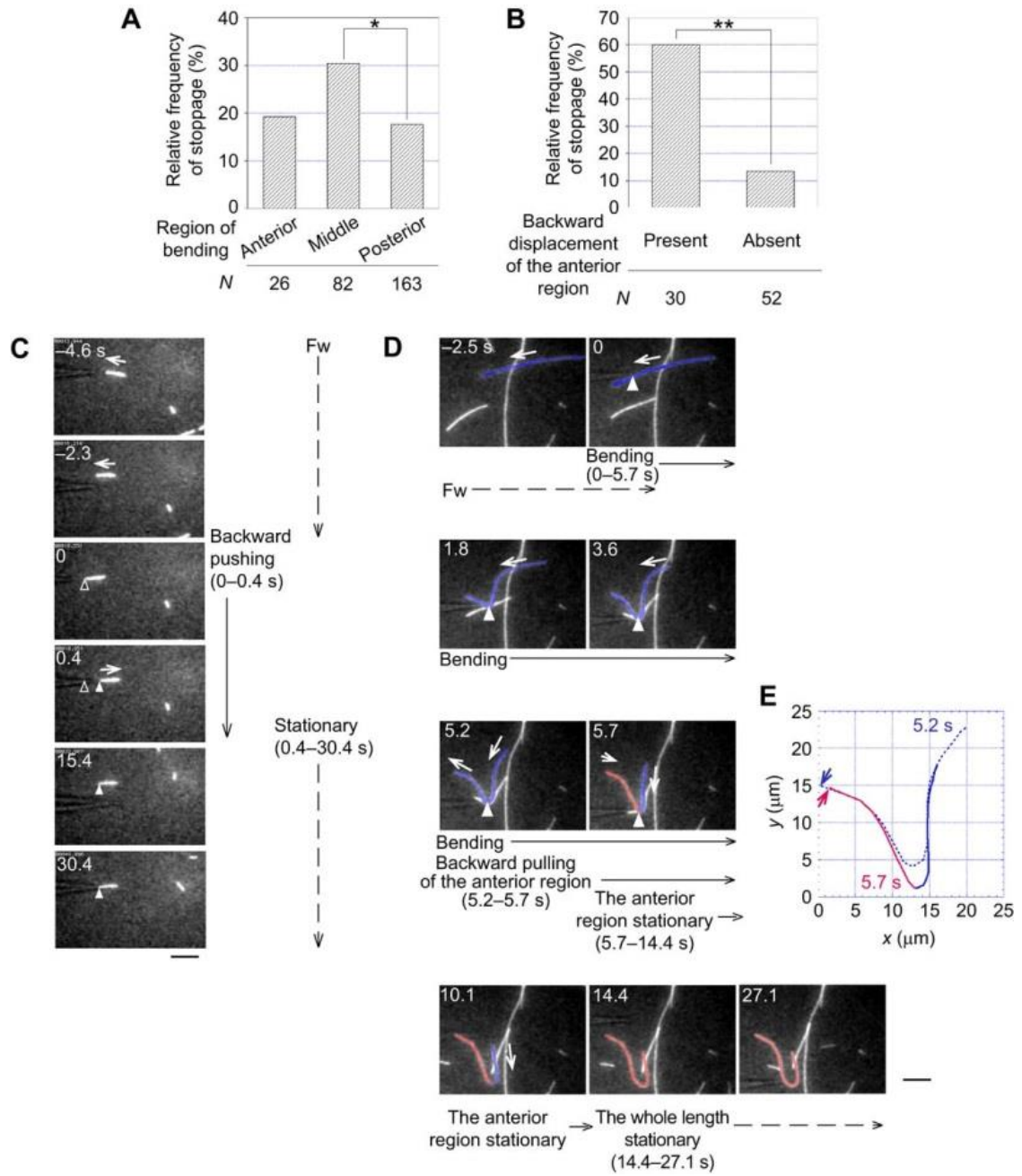


Fig. 1-7

Backward sliding was induced by continuous backward strain. (A) Sequential images of a microtubule that showed backward sliding (Bw) in the anterior region in response to continuous bending in the posterior region. The microtubule sliding towards the lower left in the panel before bending (at -5.0 s) changed its moving direction towards upper right when the posterior region was bent. Such backward sliding of the anterior region of the microtubule at 0.7 – 13.7 s was induced while the glass microneedle was kept attached to the microneedle without movement of the microneedle. After the backward movement for 13 s, the anterior region of the microtubule changed its shape with decrease in the curvature of the bend (13.7 – 46.1 s). Finally the whole microtubule recovered forward sliding (Fw) (at 50.5 s). Scale bar, 10 μm . (B) Superimposed tracings of the same microtubule shown in A (0.7 – 13.7 s). The arrowhead shows the position of the tip of the glass microneedle. The arrows show the positions of the anterior end of the microtubule and the open arrow indicates the direction of backward sliding. (C) Sequential images of a microtubule showing the backward sliding over the whole length. The microtubule was bent in the posterior region, which induced backward sliding. The glass microneedle kept attached to the microtubule seemed to slowly move towards the lower direction in the panel (1.9 – 74.9 s, the tip of the glass microneedle indicated by the arrowheads). The microtubule recovered forward sliding (original direction of movement) at 74.9 s. Scale bar, 10 μm . (D) Superimposed tracings of the same microtubule shown in C. Lines in black, blue, red and an interrupted line show, respectively, microtubule during the backward sliding at 1.9 , 28.6 , and 74.9 s and during the forward sliding at 81.3 s. The arrows indicate the positions of the both ends of the microtubule, and the open arrows indicate the direction of sliding.

Fig. 1-7

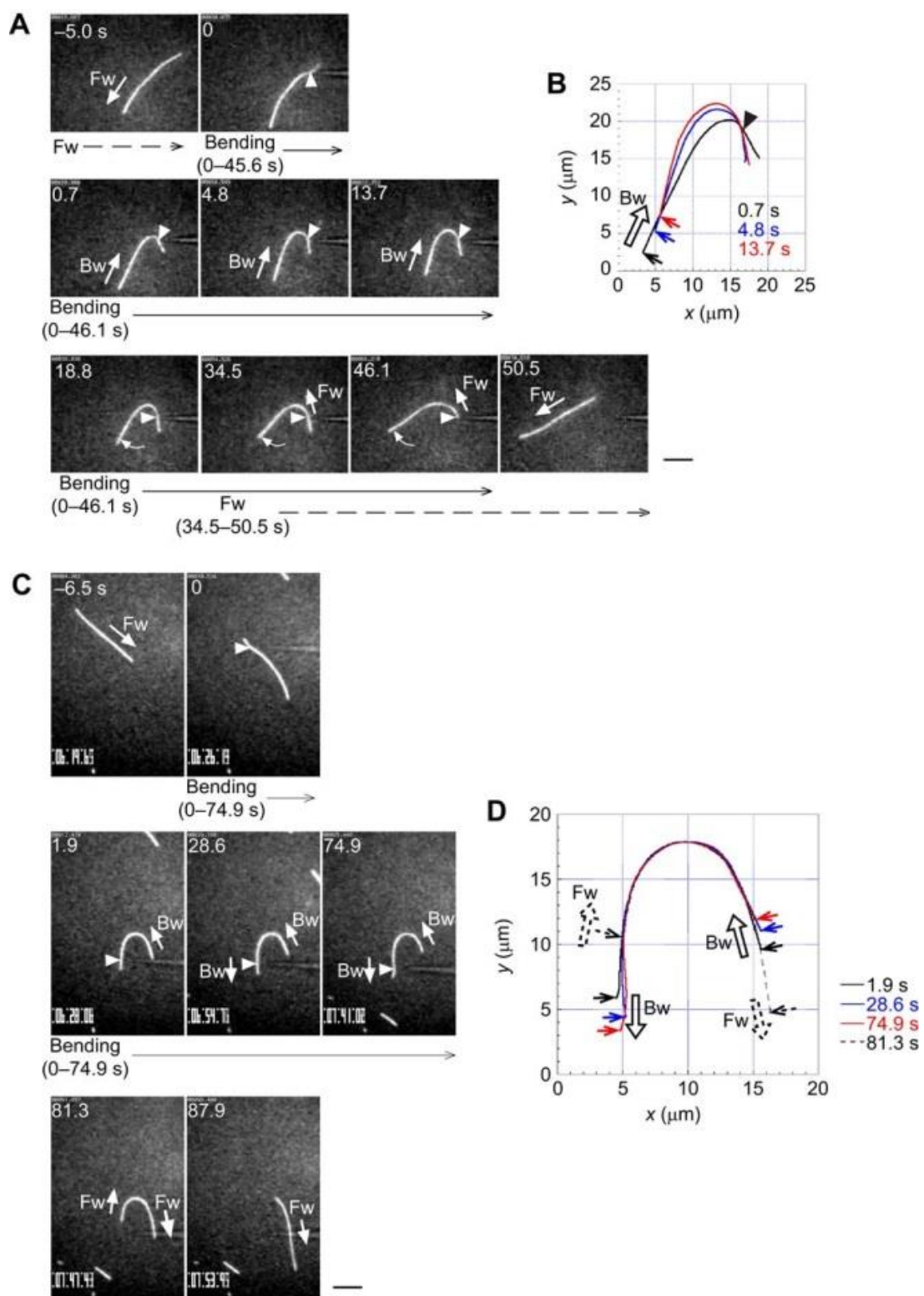


Fig. 1-8

Three-dimensional bending of the sliding microtubule caused dissociation.

Sequential images of a microtubule (MT) that showed dissociation in response to imposed bending (upper panels obtained from the record) and their schematic illustrations (lower panels). The glass microneedle was inserted into the space between the sliding microtubule and the glass surface, and resulted in a part of the microtubule being gradually blurred and difficult to focus on. Finally the whole length of the microtubule was out of focus. This indicates that the microtubule completely dissociated from the dynein-coated glass surface. Fw, forward sliding. Scale bar, 10 μm .

Fig. 1-8

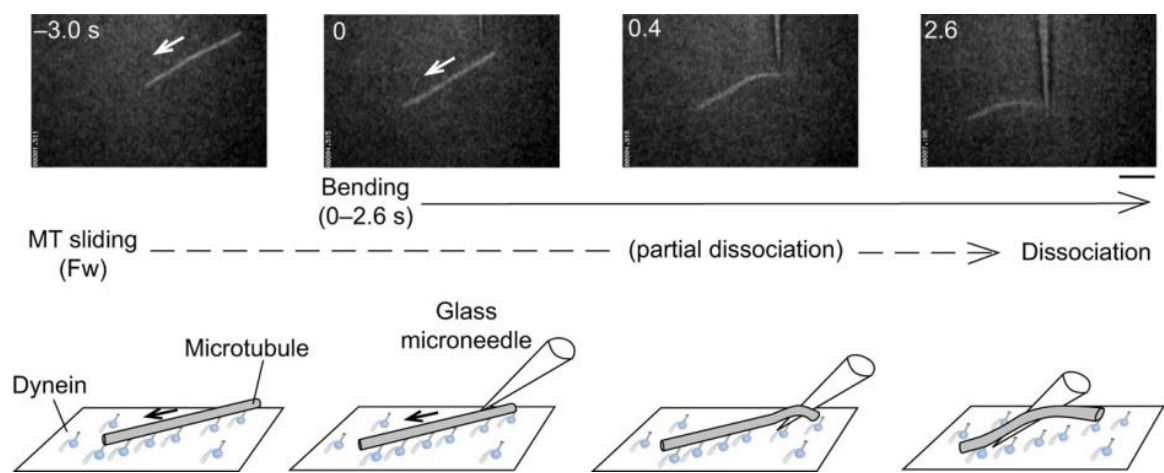
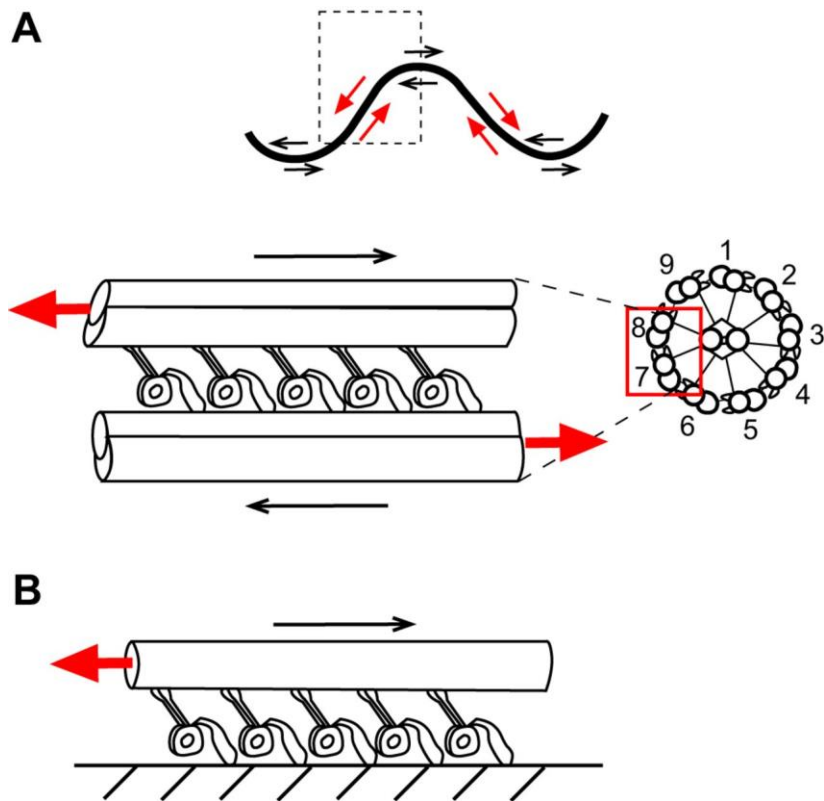


Fig. 1-9

Schematic diagrams showing the model of the regulation of dynein activities mediated by external strain. (A) Schematic depiction of the elastic strain imposed on dynein in the interbend region of a beating axoneme. Black arrows show the directions of active sliding, which mainly takes place in the bend regions to promote propagation of the bends. The upper panel shows a schematic depiction of an axoneme propagating alternate bends from the proximal (left) to the distal regions (right). As the bends propagate, dyneins in one bend region (see the middle bend, for example) eventually reach the straight interbend region (see the region indicated by the dotted rectangle), where elastic strain (red arrows) caused by the proximal bend of the axoneme is imposed on dyneins, and the reversal of the sliding direction occurs. (Note that in the leftmost bend the direction of the active sliding is the opposite to that of the middle bend.) The lower right panel shows the cross-section of the axoneme, viewed from the proximal side. The interdoubles sliding in the middle bend shown in the upper panel is thought to be produced by dyneins on the doublet number 7 (the red rectangle in the lower right panel). The lower left panel shows the directions of the active sliding (black arrows) and of the elastic strain (red arrows) imposed on the doublets 7 and 8 in the region shown by the dotted rectangle in the upper panel. (B) Schematic depiction of the backward strain that is important in inducing stoppage and backward sliding in the present experimental system. The direction of the external strain (the red arrow) relative to the direction of the active sliding (the black arrow) is the same as that of the elastic strain in the interbend region of an axoneme (A).

Fig. 1-9



Chapter II

Exploration on the method: an attempt on investigating the effects of imposed bending on the microtubule sliding induced by dyneins on the doublet microtubules

Abstract

Flagellar oscillation is based on coordinated microtubule sliding activities of ATPase motors, dyneins. Though the ATP concentration within a flagellum is kept uniformly high, sliding activities of dyneins in a flagellum are thought to be dynamically regulated through mechanical signals of bending. Whereas axonemal sub-structures such as CP and RS have been suggested to be involved in the regulation of dyneins, dyneins themselves may have the ability to respond to mechanical signals. Here, to test whether ensemble of dyneins arrayed on a doublet microtubule have the ability to modify sliding activity in response to mechanical signals directly, I studied the effects of imposed bending on the sliding movement of microtubules interacted with dyneins still attached on the doublet microtubules. At the moment, I have not found any significant differences between behaviour of the microtubules with imposed bending and that of the microtubules without one. However, I found that the relative frequency of the microtubules that showed no sliding after imposed bending was significantly higher when the anterior (leading) region of the microtubule was bent than when the middle region was bent. This result, although it is still preliminary and requires further investigation, suggests a possibility that external strain may affect the sliding activity of ensemble of dynein molecules arrayed on doublet microtubules, and that this experimental system may be useful for future studies.

Introduction

Sliding activities of dyneins in the 9+2 structure of a flagellum have been shown to be modified in response to mechanical signals, such as imposed vibration on the sperm head (Gibbons et al., 1987; Shingyoji et al., 1991), and imposed bending on the elastase-treated disintegrated axonemes (Morita and Shingyoji, 2004; Hayashi and Shingyoji, 2008). The question is whether dyneins themselves, independently from the axonemal sub-structures such as central-pair microtubules or radial spokes, have the ability to respond to mechanical signals. However, an experimental system to study the effects of external strain on the activity of dyneins arrayed on doublet microtubules independently from the axonemal sub-structures has not yet been established.

Summers and Gibbons showed that flagellar axonemes of sea urchin sperm slide apart into individual doublet microtubules with treatment by protease trypsin and by subsequent addition of 0.1 mol l^{-1} ATP (Summers and Gibbons, 1971). This suggests that the protease treatment can disrupt the inter-doublet linkages (traditionally called nexin; recently renamed as n-DRC; Heuser et al., 2009), which, in an intact axoneme, would prevent the doublets from disintegrating apart, and that the protease treatment does not disrupt the sliding ability of dyneins. Later, based on this phenomenon of sliding disintegration, an experimental system to study the activities of dyneins arrayed on a doublet microtubule was developed, in which polymerized singlet microtubules are interacted with ensemble of dyneins exposed on doublet microtubules derived from the sliding disintegration (using elastase instead of trypsin as a protease) of flagellar axonemes (Yamada et al., 1998; Yoshimura and Shingyoji, 1999). Using this assay system, the directionality and the velocity of dyneins on a doublet microtubule have

been examined in the presence of various concentrations of ATP or Ca^{2+} (Yamada et al., 1998; Yoshimura and Shingyoji, 1999; Nakano et al., 2003). However, the effect of mechanical signals on the sliding movement of the singlet microtubules in this assay system is still unknown.

Here, in order to test whether ensemble of dynein molecules can respond to mechanical signals in an independent way from the axonemal sub-structures such as central-pair microtubules, the assay system where singlet microtubules are interacted with dyneins arrayed on the doublet microtubules was modified based on the micromanipulation method described previously (Morita and Shingyoji, 2004). I have not found any significant differences between behaviour of the microtubules with imposed bending and that of the microtubules without one at the moment. However, I found that the relative frequency of the microtubules that showed no sliding after imposed bending was significantly higher when the anterior (leading) region of the microtubule was bent than when the middle region was bent. This result has not yet demonstrated the effects of imposed bending on the regulation of microtubule sliding induced by dyneins, but suggests a possibility that the sliding activity of dyneins arrayed on doublet microtubules might be affected by some kind of mechanical signals, and that this experimental system may be useful for further study.

Materials and Methods

Axonemes and microtubules

For preparation of axonemes, sperm of sea urchin, *Pseudocentrotus depressus* were suspended in 7–15 volumes of Ca²⁺-free artificial sea water (465 mmol l⁻¹ NaCl, 10 mmol l⁻¹ KCl, 25 mmol l⁻¹ MgSO₄, 25 mmol l⁻¹ MgCl₂, 2 mmol l⁻¹ Tris-HCl, pH 8.0) and demembrated with 7.5 volumes of demembrating solution [0.04% (w/v) Triton X-100, 0.15 mol l⁻¹ potassium-acetate, 2 mmol l⁻¹ MgSO₄, 2 mmol l⁻¹ EGTA, 1 mmol l⁻¹ dithiothreitol (DTT) and 10 mmol l⁻¹ Tris-HCl, pH 8.0] for 30 or 90 s at 24°C. The demembration was stopped by adding 10 volumes of Ca²⁺-free reactivating solution [0.15 mol l⁻¹ potassium-acetate, 2 mmol l⁻¹ MgSO₄, 2 mmol l⁻¹ EGTA, 1 mmol l⁻¹ DTT, 2% (w/v) polyethylene glycol (molecular weight: 20,000) and 10 mmol l⁻¹ Tris-HCl, pH 8.0] without ATP. The demembrated sperm were labelled with 6.3 μmol l⁻¹ tetramethylrhodamine (C-1171, Molecular Probes) for 4 min on ice. The labelled sperm were centrifuged at 5,300 g (3 min) and resuspended in the reactivating solution, containing 20 mmol l⁻¹ HEPES-KOH (pH 7.8) instead of Tris-HCl (pH 8.0), without ATP. The reactivating solution (HEPES, pH 7.8) was used in the following steps. For obtaining the axonemal fragments, the tetramethylrhodamine-labelled sperm were homogenized, and sperm heads were removed by centrifugation at 2,000 g (3 min); the supernatant containing axonemal fragments was centrifuged at 19,000 g (10 min) and resuspended in the reactivating solution (HEPES) without ATP. All procedures after demembration were performed at 4°C or on ice.

For singlet microtubules, see Materials and Methods in the Chapter I.

Induction of microtubule sliding on dyneins exposed on doublet microtubules

Microtubule sliding on doublet microtubules was induced according to the previous method (Yoshimura and Shingyoji, 1999) with some modifications. A suspension of tetramethylrhodamine-labelled axonemal fragments (10 μl) was introduced into a 0.5 μl perfusion chamber constructed with two different sizes of glass coverslips (24 mm \times 50 mm and 6 mm \times 18 mm) and 20 μm -thick plastic sheets used as a spacer. Reactivating solution (HEPES; 10 μl) was perfused into the chamber to wash out excess axonemes. The axonemal fragments were then treated with an elastase solution [2 $\mu\text{g ml}^{-1}$ elastase (type III, Sigma) and 5 $\mu\text{g ml}^{-1}$ soybean trypsin inhibitor (type I-S, Sigma) in reactivating solution without ATP] for 1.5 min at 22°C in the perfusion chamber. The elastase treatment was stopped with ovoidinhibitor [50 $\mu\text{g ml}^{-1}$ trypsin inhibitor from chicken egg white (type IV-O, Sigma) in reactivating solution without ATP]. This was followed by perfusion with casein solution (about 1 mg ml^{-1} casein in reactivating solution without ATP) and then, in 2 min, excess casein was washed out with reactivating solution without ATP. Next, 0.02 mmol l^{-1} ATP in reactivating solution was introduced to induce the sliding disintegration of the axonemes. This was followed by perfusion with hexokinase solution [20 units per ml hexokinase (TOYOBO, Osaka, Japan) and 50 mmol l^{-1} glucose in assay buffer], which was used to decrease the ATP concentration by hydrolysis of ATP into ADP. Assay buffer consists of 20 mmol l^{-1} HEPES, 5 mmol l^{-1} magnesium acetate, 70 mmol l^{-1} potassium acetate, 2 mmol l^{-1} EGTA, 0.1 mmol l^{-1} ethylenediamine-N, N, N', N'-tetraacetic acid-dipotassium salt, dihydrate (EDTA) and 1 mmol l^{-1} DTT. Finally, microtubules (final concentration, approximately 10 $\mu\text{g ml}^{-1}$) were introduced into the chamber, which were suspended in assay buffer to which 1 mmol l^{-1} caged ATP [P^3 -1-(2-nitrophenyl) ethyl ester of ATP,

Dojindo Laboratories, Kumamoto, Japan], 20 units per ml hexokinase, 1% (v/v) β -mercaptoethanol, 20 mmol l⁻¹ glucose, 216 μ g ml⁻¹ glucose oxidase, 36 μ g ml⁻¹ catalase and 20 μ mol l⁻¹ paclitaxel were added. To induce sliding, ATP was released from caged ATP by 60 ms-UV illumination from a mercury arc lamp (USH-102D; Ushio, Tokyo, Japan) through a 360 \pm 5 nm band pass filter and an electronic shutter. The ATP application by photolysis of caged ATP induced sliding of singlet microtubules along the doublet microtubules for only a few seconds, after which microtubules became stationary at the midst of the doublet microtubules (see the Results and Discussion). With this method one can afford enough time to apply mechanical manipulations to the microtubules interacted with dyneins on the doublet microtubules. Application of mechanical manipulations would be difficult if ATP were applied with bath application because the singlet microtubules might quickly slide until they reach the end of the doublet microtubules and dissociate in the presence of a constant concentration of ATP.

Observation of microtubule sliding, application of mechanical manipulation, and recording and analysis of response

An open surface was obtained over the microtubules based on the method of the micromanipulation assay described previously (Morita and Shingyoji, 2004). To make it possible to apply mechanical manipulation with a glass microneedle to the microtubules, 100 μ l of assay buffer [with 1 mmol l⁻¹ caged ATP, 20 units per ml hexokinase, 1% (v/v) β -mercaptoethanol, 20 mmol l⁻¹ glucose, 216 μ g ml⁻¹ glucose oxidase, 36 μ g ml⁻¹ catalase and 20 μ mol l⁻¹ paclitaxel (without microtubules)] was added on the smaller (upper) coverslip after the perfusion of the microtubules, and the smaller coverslip was

carefully slid sideways with tweezers. Microtubule sliding induced by dyneins on doublet microtubules were observed at room temperature (22°C) under an inverted fluorescence microscope equipped with a caged system (IX-70 with IX-RFA/CAGED; Olympus, Tokyo, Japan) with a $\times 100$ objective lens (NA=1.4; PlanApo; Olympus) with a mercury arc lamp (USH-102D; Ushio, Tokyo, Japan) for excitation. Tetramethylrhodamine-labelled (darker) doublet microtubules were distinguished from tetramethylrhodamine-labelled (brighter) microtubules by the brightness of the fluorescence microscope image. The glass microneedles were made with a micropipette puller (PP-830; Narishige, Tokyo, Japan) and a glass-rod (G-1000; Narishige). They were attached to and controlled by a water hydraulic micromanipulator (MW-3; Narishige), with the angle of approach to the coverslip around 20 deg. A glass microneedle was visualized simultaneously with the microtubules as a phase-contrast image using a halogen lamp for illumination. The movement of microtubules and glass microneedles were recorded with an image-intensified CCD camera (C2400-77; Hamamatsu Photonics, Shizuoka, Japan) and a hard disk drive recorder.

Movies were prepared by cropping the recorded data with NIH Image software (National Institutes of Health, Bethesda, Maryland, USA), and sequential images were prepared by capturing the movies with Image J (Ver. 1.49h; National Institutes of Health). For calculation of the sliding velocities of microtubules, the sliding distances of the anterior or posterior end of the microtubules within a certain period of time (around 1 s) during which the microtubule was sliding fairly smoothly and constantly, were measured by Image J, and the average sliding velocities during that period was calculated.

Results and Discussion

Microtubule sliding induced by dyneins arrayed on the doublet microtubules

In order to test whether ensemble of dynein molecules can respond to mechanical signals, the previously developed assay system where singlet microtubules interact with and slide on the dynein arms exposed on the disintegrated axonemes (Yamada et al., 1998; Yoshimura and Shingyoji, 1999; Nakano et al., 2003; Hayashi and Shingyoji, 2008) was modified based on the micromanipulation assay described previously (Morita and Shingyoji, 2004). Doublet microtubules were prepared by sliding disintegration of flagellar axonemes in the presence of $20 \mu\text{mol l}^{-1}$ ATP and the absence of Ca^{2+} , in which condition most axonemes disintegrate into more than three bundles of doublets or even into individual doublets (Nakano et al., 2003). By perfusion of the singlet microtubules in the presence of 1 mmol l^{-1} caged ATP, the singlet microtubules bound to dyneins on the doublet microtubules of disintegrated axonemes (-0.2 s in Fig. 2-1A). In this experimental setup, doublet microtubules retain both inner and outer arm dyneins. The singlet microtubules are interacted with either inner arm dyneins or outer arm dyneins, or both. An application of photo-released ATP from caged ATP by the 1st UV flash in the presence of hexokinase with glucose, which are used to hydrolyze and lower the concentration of released ATP, induced limited sliding of those microtubules for a few seconds ($0-4.3 \text{ s}$ in Fig. 2-1A). I term the direction of the initial sliding induced by the 1st UV flash as “forward” sliding, and the leading region of the microtubule in the 1st UV-induced sliding as the “anterior” region. In a similar axonemal situation, it has been confirmed that the forward sliding is always toward the plus end of the microtubules, namely, the anterior end is the plus end (Shingyoji et al., 1998). The average sliding

velocity was $4.3 \pm 1.6 \mu\text{m s}^{-1}$ (mean \pm s.d., $N=12$). After the sliding induced by the 1st UV flash, microtubules either slid to the end of the doublet and dissociated, or became stationary again at the midst of the doublet (as in 4.3 s in Fig. 2-1A and 3.2 s in Fig. 2-1B). Mechanical manipulation of bending with a glass microneedle was applied to those microtubules which were still attached to the doublet microtubules after the 1st UV flash (11.3–12.4 s in Fig. 2-1A), and then the movement of the bent microtubules induced by the 2nd UV flash was investigated.

Responses of the microtubules induced by the 2nd UV flash after imposed bending

Fifteen trials of bending were applied to 15 singlet microtubules (lengths: $13.3 \pm 11.7 \mu\text{m}$, mean \pm s.d., $N=15$). Bend angles, defined so that they are zero deg when the microtubules are straight, were 52 deg in average, and ranged from 13 to 85 deg ($N=14$; in one case among the 15 trials of bending, bending was applied in a three-dimensional way and the bend angle was not able to be measured.). I found that six of the microtubules with imposed bending showed forward sliding after the 2nd UV flash (Fig. 2-1A,B), while the rest (nine) of them showed no sliding after imposed bending (Fig. 2-2). The microtubules that showed no sliding after the 2nd UV flash showed neither sliding movement or diffusive motion, and stayed stationary within focus after the 2nd UV flash (Fig. 2-2), which is different from the behaviour of a microtubule that dissociated from dyneins, which show diffusive motion and come out of focus. This result suggests that the microtubules that showed no sliding after the 2nd UV flash retained interaction with dyneins on the doublet microtubules. The observation of “no sliding” after the 2nd UV flash might reflect a mode of motility of dyneins, in which dyneins crossbridge microtubules without producing sliding, even in the presence of

ATP. However, the relative frequency of the microtubules that showed no sliding after 2nd UV flash after imposed bending was not significantly different from that of the control microtubules (lengths: $9.4 \pm 7.1 \mu\text{m}$, mean \pm s.d., $N=19$) without imposed bending (chi-squared test, $P=0.85$; Fig. 2-3A). Also, there was no statistically significant difference in the sliding velocities of the microtubule sliding induced by the 2nd UV flash between the microtubules with and without imposed bending (Mann Whitney U-test, $P=0.17>0.05$; Table 2-1). Thus, I cannot conclude from the present results whether the change in modes of motility of dyneins on the doublet microtubules can be induced by imposed bending.

To obtain more information about the effects of external strain imposed by bending, I categorized the bending manipulations by the regions of bending of the singlet microtubules and quantified the relative frequencies of the microtubules that showed no sliding after the 2nd UV flash. I found that the relative frequency of the microtubules that showed no sliding after the 2nd UV was significantly higher (Fisher's exact test, $P=0.035<0.05$) when the anterior region of the microtubule was bent (80%; 8 out of 10 trials of bending) than when the middle region was bent (0%; 0 out of 3 trials of bending), although neither of those relative frequencies was significantly different (Fisher's exact test, $P>0.05$) from that of the control microtubules without bending (63%; 12 out of 19 trials of bending) (Fig. 2-3B). The sample size is not large and it still requires further investigation, but this result suggests that some kind of external strain related to imposed bending in different regions of microtubules might affect the sliding activity of ensemble of dyneins on doublet microtubules. The present result has not demonstrated the effects of imposed bending on microtubule sliding induced by dyneins on the doublet microtubules, but suggests that this experimental system may be useful

to further study the effects of external strain on microtubule sliding induced by dyneins arrayed on doublet microtubules.

Table 2-1

Sliding velocities of the singlet microtubules that showed forward sliding in response to the 2nd UV flash with and without imposed bending.

	Velocity of sliding induced by the 1st UV flash ($\mu\text{m s}^{-1}$)	Velocity of sliding induced by the 2nd UV flash ($\mu\text{m s}^{-1}$)	<i>N</i>
Microtubules with imposed bending	4.4 ± 1.8	* 3.5 ± 1.5	6
Microtubules without imposed bending	4.2 ± 1.6	* 2.8 ± 1.6	6

Mean \pm s.d. of the sliding velocities are shown. For “microtubules with imposed bending”, bending was imposed before the 2nd UV flash. *There was no statistically significant difference between the sliding velocities induced by the 2nd UV flash between microtubules with and without imposed bending (Mann-Whitney U-test, $P=0.17>0.05$). *N*, number of singlet microtubules.

Fig. 2-1

Forward sliding movements of singlet microtubules induced by photolysis of 1 mM caged ATP before and after imposed bending. (A) Sequential video images (upper row) and the traces (lower row) showing a singlet microtubule (MT) that showed forward sliding before and after imposed bending in the posterior region of the microtubule. The numbers in the upper right corner of each video image are time (s) counted after the 1st UV flash. The singlet microtubule (top left in the image at -0.2 s) slid along the doublet microtubule (DMT; labelled darker than the singlet microtubules; either a single doublet microtubule or a bundle of a few doublet microtubules) unidirectionally after the 1st UV flash (0 s) before imposed bending (11.3–12.4 s) and after the 2nd UV flash (14.3 s) after imposed bending. Arrows show the sliding direction of the singlet microtubule. The background signals are more intense at 4.3, 11.3 and 12.4 s than in other panels because of the illumination for obtaining the phase-contrast image of the microneedle. The position of the tip of the microneedle is indicated by arrowheads in video images in which bending was performed. The singlet microtubule in the left part of each panel (indicated with interrupted lines in the traces) are bound to another doublet microtubule (not shown in the images) and remained stationary. Scale bar, 10 μm . (B) Sequential video images (left column) and the traces (right column) showing a singlet microtubule that showed forward sliding before and after imposed bending in the middle region of the microtubule. Scale bar, 10 μm .

Fig. 2-1

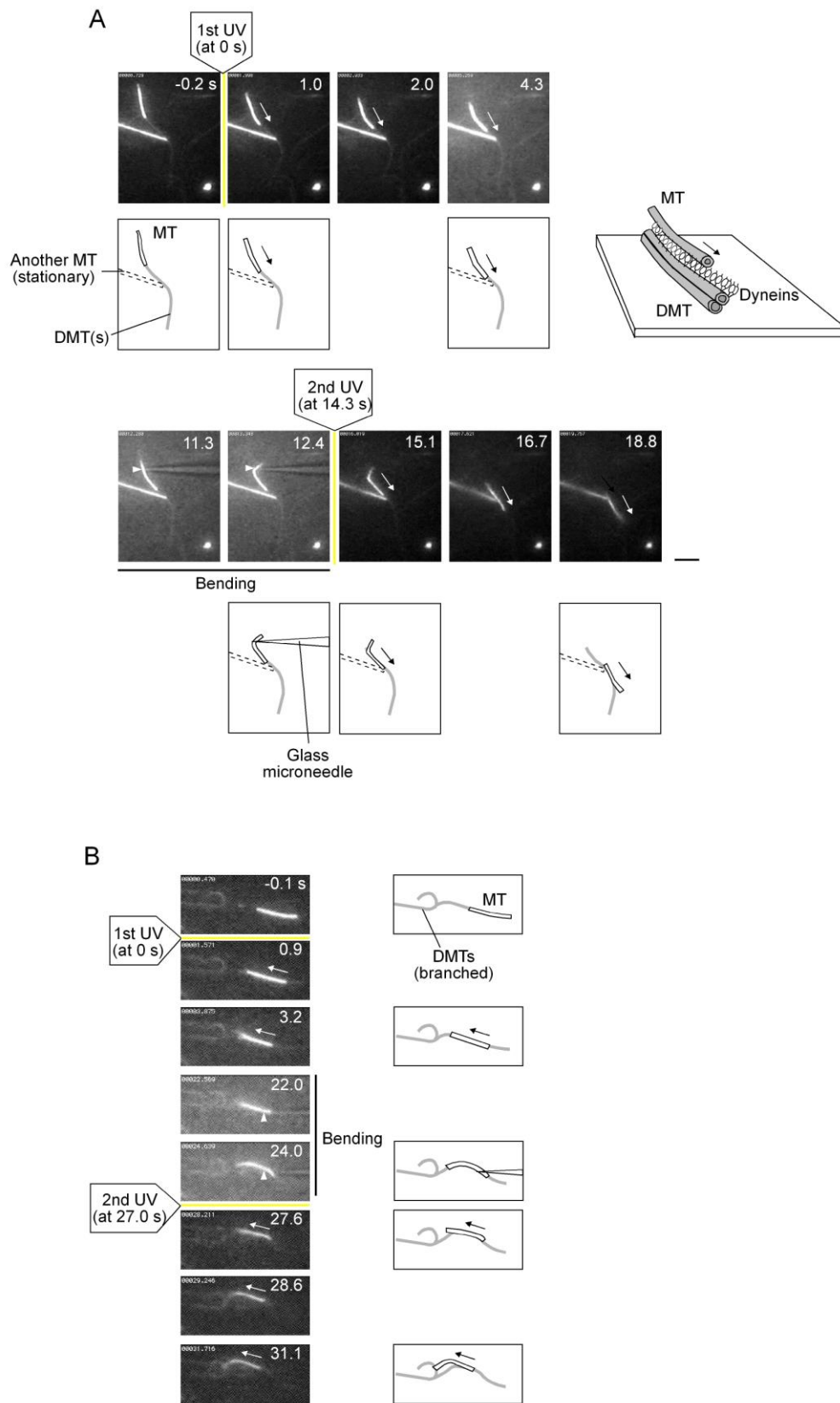


Fig. 2-2

An example of the microtubules that showed no sliding after the 2nd UV flash after imposed bending. Sequential video images (left column) and the traces (right column) of a singlet microtubule that showed forward sliding (0–3.4 s) in response to the 1st UV flash (0 s) before bending (12.6–14.4 s), but showed no sliding after the 2nd UV flash (16.7 s) after imposed bending in the anterior region of the microtubule. The position of the tip of the glass microneedle is indicated by filled arrowheads in video images at 12.6 and 14.4 s. The position of the anterior end of the singlet microtubule at 17.7 s is shown by open arrowheads in video images at 17.7 and 18.8 s. The glass microneedle is visible only while the illumination for the phase-contrast image was used (12.6 and 14.4 s), but the position of the microneedle was unchanged after 14.4 s, keeping the bend of the microtubule (see the trace at 18.8 s). MT, singlet microtubule. DMT, doublet microtubule. Scale bar, 10 μm .

Fig. 2-2

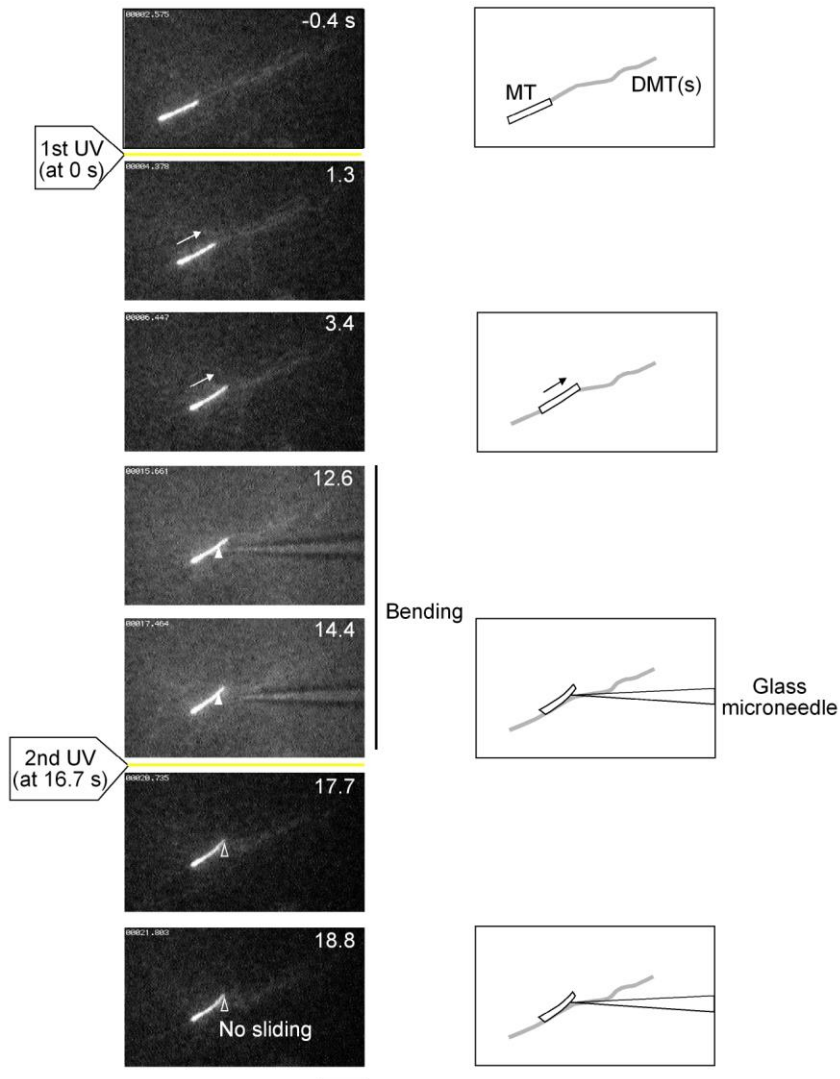
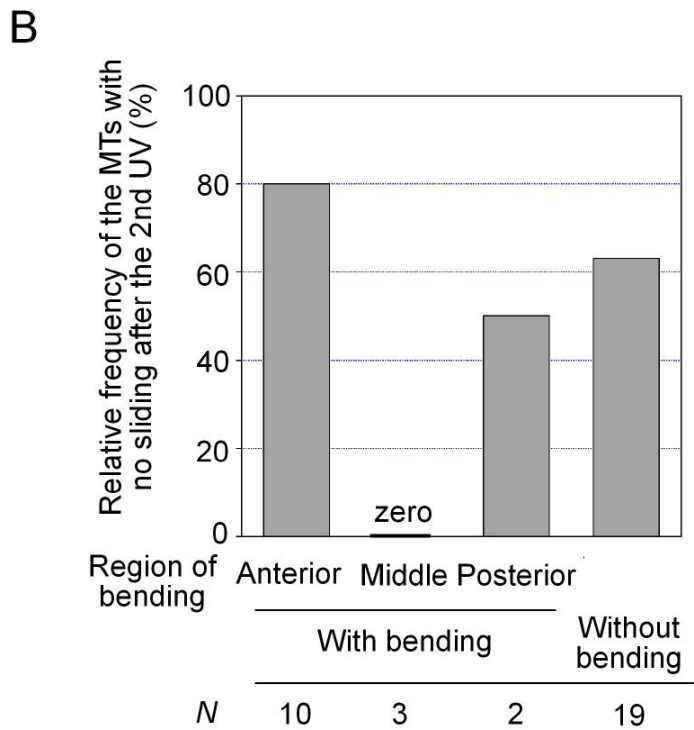
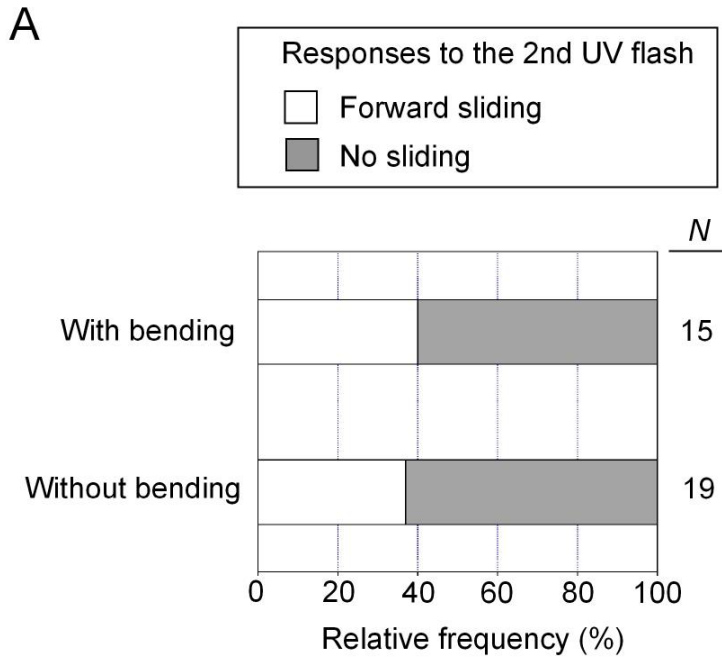


Fig. 2-3

Relative frequencies of responses of the singlet microtubules to the 2nd UV flash after imposed bending and the effect of the regions of bending. (A) Relative frequencies of responses of the singlet microtubules (that showed sliding in response to the 1st UV flash before imposed bending) to the 2nd UV flash after imposed bending. “Without bending” shows the responses of the control microtubules, which showed sliding in response to the 1st UV flash and did not dissociate from the doublet microtubule, and which were not mechanically manipulated. N , number of singlet microtubules. (B) Relative frequencies of the microtubules that showed no sliding in response to the 2nd UV flash after imposed bending in different regions of the singlet microtubules. N , number of singlet microtubules.

Fig. 2-3



General Discussion

In this thesis, to test whether ensemble of dynein molecules have the ability to respond to mechanical signals, effects of external strain on microtubule sliding induced by ensemble of dyneins were investigated. In the Chapter I, microtubule sliding induced by isolated outer arm dyneins adsorbed on a glass surface was investigated. I found that planar bending can induce three different modes of motility of dynein: continuation of forward sliding, stoppage of sliding and backward sliding. Decrease in sliding velocity was also induced by planar bending. For induction of the stoppage and backward sliding, the importance of backward strain is suggested. Moreover, imposed bending with a three-dimensional effect induced dissociation of the microtubules from dyneins. In the Chapter II, I explored on another experimental system in which microtubules are interacted with dyneins still attached on doublet microtubules of a sperm flagellar axoneme, which is closer to the *in vivo* situation than the system with isolated dyneins on a glass surface. Although there has been no significant difference between behaviour of the microtubules with imposed bending and without one, I found that imposed bending in different regions of microtubules may affect the relative frequencies of the microtubules that do not show sliding in response to application of ATP.

Limitations and possible future improvements of the experimental setups

The present results in the Chapter I suggest that sliding activities of ensemble of isolated outer arm dyneins on a glass surface can be modified by external strain. Although this is a novel *in vitro* experimental system, attention should be paid to some limitations of the experimental setup. First, bending a microtubule interacted with dyneins on the glass surface inevitably shifts the position of the microtubule from the original points, therefore the set of dynein molecules interacting the microtubule would change at least

partly through imposed bending. This might make it difficult to impose effective strain to dyneins interacted with the microtubules. Secondly, dyneins are adsorbed to a glass surface and not attached to the doublet microtubules as in the axonemes. This difference in the conditions of attachment in the tail region of dyneins might affect dynein activities. Thirdly, dyneins on the glass surface are not uniformly oriented like dyneins on the doublet microtubules, but supposed to be oriented in random directions. This may lower the likelihood of the dyneins receiving effective strain through the microtubules. These limitations of the experimental setup may account for the fact that majority (76%) of the trials of planar bending resulted in continuation of forward sliding without any response (see the Results in the Chapter I).

In the experimental setup that was explored in the Chapter II, dyneins are still attached to doublet microtubules, and thus the situation is closer to the *in vivo* flagella. However, the effects of external strain have not been clearly detected in the experimental setups in the Chapter II. This may be partly because of shortage in the sample size (see Fig. 2-3B and the Results in Chapter II) and may also be because an effective way of mechanical manipulation for inducing responses of dyneins has not been established yet. The results of the experiments using isolated dyneins (Chapter I) suggested the importance of backward strain in inducing stoppage and backward sliding. Therefore, it can be hypothesized that backward strain imposed to dyneins might induce cessation of sliding or backward sliding also in dyneins still attached to doublet microtubules. The experimental system explored in the Chapter II may be useful to test this hypothesis in future studies. For example, investigating the effect of imposed bending in the anterior region of the singlet microtubules without bending the doublet microtubules may give insights on the effects of backward strain on dyneins arrayed on

the doublet microtubules. To realize imposed bending on the singlet microtubules alone without bending the doublet microtubules, discrimination of the singlet and the doublet microtubules using two different fluorescent dyes with different emission spectra may be helpful. In the present experimental condition, both of the singlet and the doublet microtubules were labelled with tetramethylrhodamine and they were distinguished by the difference in the brightness of the fluorescent signals, therefore the doublet microtubules, which were labelled darker, were often not clearly seen during micromanipulations (e.g. at 12.6 and 14.4 s in Fig. 2-2).

The modes of motility of dyneins

In beating flagella, the activities of dynein are not uniform. In sea urchin sperm, dyneins on the doublets on both sides of the CP (doublets number 3 and 7; see the lower right panel of Fig. 1-9A) mainly contribute to active sliding, and dyneins on other doublet microtubules are thought to be less active, contributing to producing stable crossbridges among the doublet microtubules (Nakano et al., 2003). Also, activities of dyneins on the doublets on both sides of the CP are thought to be alternatively switching, thus contributing to alternative bending motion of the axoneme (Hayashi and Shingyoji, 2008). Many mathematical models have presumed that dyneins on doublets on both sides of the CP are detached from the adjacent doublet microtubule when they are not active (Lindemann, 1994a; Lindemann, 1994b; Brokaw, 1975; Riedel-Kruse et al., 2007). However, it is also possible that dyneins can adopt modes of motility other than the forward sliding mode without detachment from the adjacent microtubule. For example, when the active arrays of dyneins are switched from the dyneins on the doublet number 7 to those on the doublet number 3, the dyneins on the doublet number

7 may temporarily adopt the stationary mode without detachment from the adjacent microtubule. Also, there is a possibility that dyneins on the doublet number 3 (or 7) contribute to backward sliding while dyneins on the doublet number 7 (or 3), which is in the opposite side of the CP, are in the forward sliding mode. The existence of backward sliding mode in dyneins on doublet number 7 (or 3) could contribute to the stability of a beating axoneme because it could prevent the twist of the axoneme that could be generated by active forward shear force exerted by dyneins on the doublet number 3 (or 7) (Hines and Blum, 1985; Brokaw, 2009). And importantly, backward stepping and backward force generation have been induced by external strain in single-molecule assays (Shingyoji et al., 1998; Shingyoji et al., 2015).

The present results in the Chapter I demonstrate that ensemble of dyneins do have the ability to adopt several modes of motility without detachment from the microtubules in the presence of physiological concentration (1 mmol l^{-1}) of ATP: the forward sliding mode, the stationary mode, and the backward sliding mode. The present results also suggest that changes of modes of motility do not require axonemal sub-structures such as CP and RS, but are induced by mechanical signals imposed on dyneins themselves. The present results suggest that this regulatory mechanism of the modes of motility through mechanical signals may also be present in a beating axoneme as the regulation through shear strain such as elastic strain resulting from the bends of an axoneme (see the Discussion of the Chapter I), which may be an important basis of the flagellar oscillation.

Coordination of dynein activities through mechanical signals

The responses induced by external strain in the behaviour of microtubules interacted by

ensemble of dyneins in this thesis suggest that collective activities of ensemble of dynein molecules can be regulated and coordinated directly by mechanical signals, at least for purified outer arm dyneins adsorbed on a glass surface (the Chapter I), and perhaps for dyneins still attached on doublet microtubules (the Chapter II).

In this thesis, outer arm dyneins from sea urchin sperm were used in the Chapter I, and dyneins including both inner and outer arms on the doublet microtubules of sea urchin sperm were used in the Chapter II. The effects of external strain on the activities of inner arm dyneins have not been thoroughly investigated, but it has been suggested that inner arm dynein subspecies f of *Chlamydomonas* seem to accelerate dissociation from the microtubules in response to strain (Kotani et al., 2007), and the effects of external strain on the activities of inner arm dyneins can be investigated in future studies using the experimental systems developed in this thesis, either by using isolated *Chlamydomonas* inner arm dyneins (Sakakibara et al., 1999; Kotani et al., 2007) instead of sea urchin outer arm dyneins in the experimental system developed in the Chapter I, or by using outer arm-extracted sea urchin sperm axonemes (Gibbons and Gibbons, 1973) in the experimental system developed in the Chapter II. The properties of responses of outer arms and inner arms may be different, but regulation through mechanical signals may be a common feature of both outer and inner arm dyneins underlying the emergence of flagellar oscillation.

Central-pair microtubules are likely to be involved in the regulation of dynein activities through mechanical signals, particularly in determination of the beat plane through activation of dyneins on doublets on both sides of the central-pair microtubules, which are considered to rotate in response to external strain (Gibbons et al., 1987; Nakano et al., 2003). It seems likely that the direct regulatory mechanism of dynein

activity through mechanical signals of bending, as proposed in this thesis, is important in production of the regular bending movement of the axoneme within the beat plane prescribed by the central-pair.

Regulation through mechanical signals has also been reported on the activities of cytoplasmic dyneins. A single molecule analysis of cytoplasmic dynein has revealed that backward strain induces more frequent backward stepping (Gennerich et al., 2007). Also, it has been reported that multiple of dynein molecules bind tenaciously to microtubules in response to large backward strain (Leidel et al., 2012; Rai et al., 2013). Coordination of activities through mechanical signals might be a common feature of both axonemal and cytoplasmic dyneins. The experimental systems developed in this thesis may be useful to investigate the effects of mechanical signals on the activities of ensemble of motor proteins in general, including outer arm dyneins, inner arm dyneins, and cytoplasmic dyneins.

Conclusion

Activities of dyneins in a beating flagellum seem to change dynamically in a coordinated manner. Such alternations include changes in velocity, and possibly include transitions among modes of motility such as forward sliding mode, production of stable crossbridges, backward sliding mode and dissociation from the microtubules. In this thesis, two experimental systems to investigate the effects of external strain on the activities of ensemble of dyneins were developed. The present results suggest that ensemble of dyneins have the ability to modify the sliding activities in a flexible manner in an independent mechanism from axonemal sub-structures such as CP and RS, and

that external strain can play the role of coordinating the activities of multiple molecules of dyneins along a microtubule. This regulatory mechanism may be an important aspect of the communication within an axoneme underlying the emergence of oscillatory movement of cilia and flagella. The relationship between this shear strain-dependent regulatory mechanism and other kinds of regulation, such as nucleotide-dependent regulation (Inoue and Shingyoji, 2007; Yoshimura et al., 2007), regulation by transverse force (Lindemann, 1994a,b; Lindemann and Lesich, 2015) and Ca^{2+} ion (Brokaw, 1979) is a remaining problem for future studies.

References

- Alper, J. D., Tovar, M. and Howard, J.** (2013). Displacement-weighted velocity analysis of gliding assays reveals that *Chlamydomonas* axonemal dynein preferentially moves conspecific microtubules. *Biophys. J.* **104**, 1989-1998.
- Bradford, M. M.** (1976). A rapid and sensitive method for the quantitation of microgram quantities of protein utilizing the principle of protein-dye binding. *Anal. Biochem.* **72**, 248-254.
- Brokaw, C. J.** (1975). Molecular mechanism for oscillation in flagella and muscle. *Proc. Natl. Acad. Sci. USA.* **72**, 3102-3106.
- Brokaw, C. J.** (1979). Calcium-induced asymmetrical beating of triton-demembrated sea urchin sperm flagella. *J. Cell Biol.* **82**, 401-411.
- Brokaw, C. J.** (1989). Direct measurements of sliding between outer doublet microtubules in swimming sperm flagella. *Science* **243**, 1593-1596.
- Brokaw, C. J.** (1994). Control of flagellar bending: a new agenda based on dynein diversity. *Cell Motil. Cytoskeleton* **28**:199-204.
- Brokaw, C. J.** (1999). Computer simulation of flagellar movement: VII. Conventional but functionally different cross-bridge models for inner and outer arm dyneins can explain the effects of outer arm dynein removal. *Cell Motil. Cytoskeleton* **42**, 134-148.
- Brokaw, C. J.** (2001). Simulating the effects of fluid viscosity on the behaviour of sperm flagella. *Mathematical Methods In The Applied Sciences* **24**, 1351-1365.
- Brokaw, C. J.** (2009). Thinking about flagellar oscillation. *Cell Motil. Cytoskeleton* **66**, 425-436.
- Brokaw, C. J. and Gibbons, I. R.** (1975). Mechanisms of movement in flagella and cilia. In *Swimming and Flying in Nature*, Vol. I (ed. WU, T. Y.-T., BROKAW, C.

J. and BRENNAN, C.), pp. 89-126. New York: Plenum.

Brokaw, C. J. and Kamiya, R. (1987). Bending patterns of *Chlamydomonas* flagella: IV. Mutants with defects in inner and outer dynein arms indicate differences in dynein arm function. *Cell Motil. Cytoskeleton* **8**, 68-75.

Castoldi, M. and Popov, A. V. (2003). Purification of brain tubulin through two cycles of polymerization-depolymerization in a high-molarity buffer. *Protein Expr. Purif.* **32**, 83-88.

Fox, L. A. and Sale, W. S. (1987). Direction of force generated by the inner row of dynein arms on flagellar microtubules. *J. Cell Biol.* **105**, 1781-1787.

Frey, E., Brokaw, C. J. and Omoto, C. K. (1997). Reactivation at low ATP distinguishes among classes of paralyzed flagella mutants. *Cell Motil. Cytoskeleton* **38**, 91-99.

Fridman, V., Gerson-Gurwitz, A., Shapira, O., Movshovich, N., Lakamper, S., Schmidt, C. F. and Gheber, L. (2013). Kinesin-5 Kip1 is a bi-directional motor that stabilizes microtubules and tracks their plus-ends in vivo. *J. Cell Sci.* **126**, 4147-4159.

Gennerich, A., Carter, A. P., Reck-Peterson, S. L. and Vale, R. D. (2007). Force-induced bidirectional stepping of cytoplasmic dynein. *Cell* **131**, 952-965.

Gibbons, B. H. and Gibbons, I. R. (1972). Flagellar movement and adenosine triphosphatase activity in sea urchin sperm extracted with Triton X-100. *J. Cell Biol.* **54**, 75-97.

Gibbons, B. H. and Gibbons, I. R. (1973). The effect of partial extraction of dynein arms on the movement of reactivated sea-urchin sperm. *J. Cell Sci.* **13**, 337-357.

Gibbons, I. R. (1981). Transient flagellar waveforms during intermittent swimming in

- sea urchin sperm. II. Analysis of tubule sliding. *J. Muscle Res. Cell Motil.* **2**, 83-130.
- Gibbons, I. R. and Rowe, A. J.** (1965). Dynein: A Protein with Adenosine Triphosphatase Activity from Cilia. *Science* **149**, 424-426.
- Gibbons, I. R., Shingyoji, C., Murakami, A. and Takahashi, K.** (1987). Spontaneous recovery after experimental manipulation of the plane of beat in sperm flagella. *Nature* **325**, 351-352.
- Goldstein, S. F.** (1977). Asymmetric waveforms in echinoderm sperm flagella. *J. Exp. Biol.* **71**, 157-170.
- Hamasaki, T., Holwill, M. E. J., Barkalow, K. and Satir, P.** (1995). Mechanochemical aspects of axonemal dynein activity studied by *in vitro* microtubule translocation. *Biophys. J.* **69**, 2569-2579.
- Hayashi, S., and Shingyoji, C.** (2008). Mechanism of flagellar oscillation – bending-induced switching of dynein activity in elastase-treated axonemes of sea urchin sperm. *J. Cell Sci.* **121**, 2833-2843.
- Heuser, T., Raytchev, M., Krell, J., Porter, M. E. and Nicastro, D.** (2009). The dynein regulatory complex is the nexin link and a major regulatory node in cilia and flagella. *J. Cell Biol.* **187**, 921-933.
- Hines, M., and Blum, J. J.** (1985). On the contribution of dynein-like activity to twisting in a three-dimensional sliding filament model. *Biophys. J.* **47**, 705-708.
- Hirakawa, E., Higuchi, H. and Toyoshima, Y. Y.** (2000). Processive movement of single 22S dynein molecules occurs only at low ATP concentrations. *Proc. Natl. Acad. Sci. USA.* **97**, 2533-2537.
- Hosokawa, Y. and Miki-Noumura, T.** (1987). Bending motion of *Chlamydomonas*

- axonemes after extrusion of central-pair microtubules. *J. Cell Biol.* **105**, 1297-1301.
- Hyman, A., Drechsel, D., Kellogg, D., Salser, S., Sawin, K., Steffen, P., Wordeman, L. and Mitchison, T.** (1991). Preparation of modified tubulins. *Methods Enzymol.* **196**, 478-485.
- Imai, H. and Shingyoji, C.** (2003). Effects of trypsin-digested outer-arm dynein fragments on the velocity of microtubule sliding in elastase-digested flagellar axonemes. *Cell Struct. Funct.* **32**, 17-27.
- Inoue, Y. and Shingyoji, C.** (2007). The roles of noncatalytic ATP binding and ADP binding in the regulation of dynein motile activity in flagella. *Cell Motil. Cytoskeleton* **64**, 690-704.
- Kikushima, K. and Kamiya, R.** (2009). Ratchetlike properties of *in vitro* microtubule translocation by *Chlamydomonas* inner-arm dynein species c in the presence of flow. *Biophys. J.* **97**, 1657-1662.
- Kotani, N., Sakakibara, H., Burgess, S. A., Kojima, H. and Oiwa, K.** (2007). Mechanical properties of dynein-f (dynein II) studied with *in vitro* motility assays. *Biophys. J.* **93**, 886-894.
- Kron, S. J., and Spudich, J. A.** (1986). Fluorescent actin filaments move on myosin fixed to a glass surface. *Proc. Natl. Acad. Sci. USA.* **83**, 6272-6276.
- Leidel, C., Longoria, R. A., Gutierrez, F. M. and Shubeita, G. T.** (2012). Measuring molecular motor forces *in vivo*: implications for tug-of-war models of bidirectional transport. *Biophys. J.* **103**, 492-500.
- Lindemann, C. B.** (1994a). A “geometric clutch” hypothesis to explain oscillations of the axoneme of cilia and flagella. *J. Theor. Biol.* **168**, 175-189.

- Lindemann, C. B.** (1994b). A model of flagellar and ciliary functioning which uses the forces transverse to the axoneme as the regulator of dynein activation. *Cell Motil. Cytoskeleton* **29**, 141-154.
- Lindemann, C. B.** (2014) Dynein regulation: going into circles can set things straight. *Biophys. J.* **106**, 2285-2287.
- Lindemann, C. B. and Lesich, K. A.** (2015). The geometric clutch at 20: stripping gears or gaining traction? *Reproduction* **150**, R45-53.
- Meijering, E., Dzyubachyk, O. and Smal, I.** (2012). Methods for cell and particle tracking. In *Methods in Enzymology* Volume 504 (ed. P. M. Conn), pp. 183-200. San Diego, California: Elsevier, Inc.
- Morita, Y. and Shingyoji, C.** (2004). Effects of imposed bending on microtubule sliding in sperm flagella. *Curr. Biol.* **14**, 2113-2118.
- Moss A. G., Gatti, J. L. and Witman, G. B.** (1992). The motile β /IC1 subunit of sea urchin sperm outer arm dynein does not form a rigor bond. *J. Cell Biol.* **118**, 1177-1188.
- Mukundan, V., Sartori, P., Geyer, V. F., Julicher, F. and Howard, J.** (2014). Motor regulation results in distal forces that bend partially disintegrated *Chlamydomonas* axonemes into circular arcs. *Biophys. J.* **106**, 2434-2442.
- Nakano, I., Kobayashi, T., Yoshimura, M. and Shingyoji, C.** (2003). Central-pair-linked regulation of microtubule sliding by calcium in flagellar axonemes. *J. Cell Sci.* **116**, 1627-1636.
- Nonaka, S., Tanaka, Y., Okada, Y., Takeda, S., Harada, A., Kanai, Y., Kido, M., and Hirokawa, N.** (1998). Randomization of left-right asymmetry due to loss of nodal cilia generating leftward flow of extraembryonic fluid in mice lacking

- KIF3B motor protein. *Cell* **95**, 829-837.
- Oda, T., Yanagisawa, H., Yagi, T. and Kikkawa, M.** (2014). Mechanosignaling between central apparatus and radial spokes controls axonemal dynein activity. *J. Cell Biol.* **204**, 807-819.
- Okuno, M. and Hiramoto, Y.** (1976). Mechanical stimulation of starfish sperm flagella. *J. Exp. Biol.* **65**, 401-413.
- Omoto, C. K., Yagi, T., Kurimoto, E. and Kamiya, R.** (1996). Ability of paralyzed flagella mutants of *Chlamydomonas* to move. *Cell Motil. Cytoskeleton* **33**, 88-94.
- Paschal, B. M., King, S. M., Moss, A. G., Collins, C. A., Vallee, R. B. and Witman, G. B.** (1987). Isolated flagellar outer arm dynein translocates brain microtubules *in vitro*. *Nature* **330**, 672-674.
- Porter, M. F. and Sale, W. S.** (2000). The 9+2 axoneme anchors multiple inner arm dyneins and a network of kinases and phosphatases that control motility. *J. Cell Biol.* **151**, F37-F42.
- Prensier, G., Vivier, E., Goldstein, S. and Schrevel, J.** (1980). Motile flagellum with “3+0” ultrastructure. *Science* **207**, 1493-1494.
- Rai, A. K., Rai, A., Ramaiya, A. J., Jha, R. and Mallik, R.** (2013). Molecular adaptations allow dynein to generate large collective forces inside cells. *Cell* **152**, 172-182.
- Riedel-Kruse, I. H., Hilfinger, A., Howard, J. and Jülicher, F.** (2007). How molecular motors shape the flagellar beat. *HFSP J.* **1**, 192-208.
- Roostalu, J., Hentrich, C., Bieling, P., Telley, I. A., Schiebel, E. and Surrey, T.** (2011). Directional switching of the kinesin Cin8 through motor coupling.

Science **332**, 94-99.

- Sakakibara, H., Kojima, H., Sakai, Y., Katayama, E. and Oiwa, K.** (1999). Inner-arm dynein c of *Chlamydomonas* flagella is a single-headed processive motor. *Nature* **400**, 586-590.
- Sale, W. S. and Satir, P.** (1977). Direction of active sliding of microtubules in *Tetrahymena* cilia. *Proc. Natl. Acad. Sci. USA.* **74**, 2045-2049.
- Satir, P.** (1968). Studies on cilia 3. Further studies on the cilium tip and a “sliding filament” model of ciliary motility. *J. Cell Biol.* **39**, 77-94.
- Shiba, K., Mogami, Y. and Baba, S. A.** (2002). Ciliary movement of sea-urchin embryos. *Natural Science Report, Ochanomizu University* **53**, 49-54.
- Shingyoji, C.** (2017). Regulation of dynein-driven ciliary and flagellar movement. In *Dyneins: Structure, Biology and Disease (2nd edition)*, in press. Amsterdam, The Netherlands: Elsevier Inc.
- Shingyoji, C., Murakami, A. and Takahashi, K.** (1977). Local reactivation of Triton-extracted flagella by iontophoretic application of ATP. *Nature* **265**, 269-270.
- Shingyoji, C., Gibbons, I. R., Murakami, A. and Takahashi, K.** (1991). Effect of imposed head vibration on the stability and waveform of flagellar beating in sea urchin spermatozoa. *J. Exp. Biol.* **156**, 63-80.
- Shingyoji, C., Higuchi, H., Yoshimura, M., Katayama, E. and Yanagida, T.** (1998). Dynein arms are oscillating force generators. *Nature* **393**, 711-714.
- Shingyoji, C., Nakano, I., Inoue, Y. and Higuchi, H.** (2015). Dynein arms are strain-dependent direction-switching force generators. *Cytoskeleton* **72**, 388-401.
- Smith, E. F.** (2002). Regulation of flagellar dynein by the axonemal central apparatus.

- Cell Motil. Cytoskeleton* **52**, 33-42.
- Smith, E. F. and Sale, W. S.** (1992). Regulation of dynein-driven microtubule sliding by the radial spokes in flagella. *Science* **257**, 1557-1559.
- Summers, K. E. and Gibbons, I. R.** (1971). Adenosine triphosphate-induced sliding of tubules in trypsin-treated flagella of sea-urchin sperm. *Proc. Natl. Acad. Sci. USA*. **68**, 3092-3096.
- Vale, R. D. and Toyoshima, Y. Y.** (1988). Rotation and translocation of microtubules *in vitro* induced by dyneins from *Tetrahymena* cilia. *Cell* **52**, 459-469.
- Vale, R. D., Schnapp, B. J., Reese, T. S. and Sheetz, M. P.,** (1985). Organelle, bead, and microtubule translocations promoted by soluble factors from the squid giant axon. *Cell* **40**, 559-569.
- Vale, R. D., Soll, D. R. and Gibbons, I. R.** (1989). One-dimensional diffusion of microtubules bound to flagellar dynein. *Cell* **59**, 915-925.
- Wargo, M. J. and Smith, E. F.** (2003). Asymmetry of the central apparatus defines the location of active microtubule sliding in *Chlamydomonas* flagella. *Proc. Natl. Acad. Sci. USA*. **100**, 137-142.
- Yagi, T. and Kamiya, R.** (2000). Vigorous beating of *Chlamydomonas* axonemes lacking central pair/radial spoke structures in the presence of salts and organic compounds. *Cell Motil. Cytoskeleton* **46**, 190-199.
- Yamada, A., Yamaga, T., Sakakibara, H., Nakayama, H. and Oiwa, K.** (1998). Unidirectional movement of fluorescent microtubules on rows of dynein arms of disintegrated axonemes. *J. Cell Sci.* **111**, 93-98.
- Yoke, H. and Shingyoji, C.** (2017). Effects of external strain on the regulation of microtubule sliding induced by outer arm dynein of sea urchin sperm flagella. *J.*

Exp. Biol. **220**, 1122-1134.

Yoshimura, A., Nakano, I. and Shingyoji, C. (2007). Inhibition by ATP and activation by ADP in the regulation of flagellar movement in sea urchin sperm. *Cell Motil. Cytoskeleton* **64**, 777-793.

Yoshimura, M. and Shingyoji, C. (1999). Effects of the central pair apparatus on microtubule sliding velocity in sea urchin sperm flagella. *Cell Struct. Funct.* **24**, 43-54.